



To Deep Learn or not Deep Learning

Computational Pathology for Precision Medicine

Anant Madabhushi, PhD

Donnell Institute Professor and Director

Center for Computational Imaging and Personalized Diagnostics

Biomedical Engineering Department

Case Western Reserve University

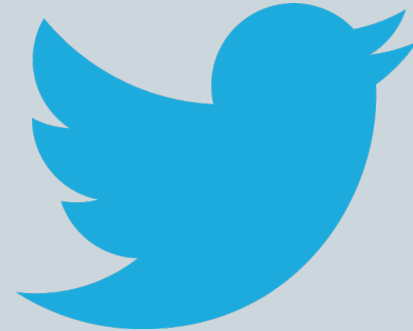
Research Health Scientist

Louis Stokes Cleveland Veterans Administration Medical Center



Anant Madabhushi

2,015 Tweets



[Edit profile](#)

Anant Madabhushi

@anantm

Artificial Intelligence, Cancer imaging, Digital pathology, radiomics, pathomics, precision medicine

@anantm

Probability of Developing Invasive Cancer during Lifetime (2019)

	Male	Female
All sites†	1 in 2	1 in 3
Breast		1 in 8
Colon & rectum	1 in 23	1 in 25
Kidney & renal pelvis	1 in 46	1 in 82
Leukemia	1 in 54	1 in 77
Lung & bronchus	1 in 15	1 in 17
Melanoma of the skin‡	1 in 28	1 in 41
Non-Hodgkin lymphoma	1 in 41	1 in 52
Prostate	1 in 9	
Thyroid	1 in 144	1 in 52
Uterine cervix		1 in 159
Uterine corpus		1 in 33

Source: DevCan: Probability of Developing or Dying of Cancer Software, Version 6.7.7. Statistical Research and Applications Branch, National Cancer Institute, 2019.

Estimated Cancer Deaths in the US, 2020

Male		Female			
Lung & bronchus	72,500	23%	Lung & bronchus	63,220	22%
Prostate	33,330	10%	Breast	42,170	15%
Colon & rectum	28,630	9%	Colon & rectum	24,570	9%
Pancreas	24,640	8%	Pancreas	22,410	8%
Liver & intrahepatic bile duct	20,020	6%	Ovary	13,940	5%
Leukemia	13,420	4%	Uterine corpus	12,590	4%
Esophagus	13,100	4%	Liver & intrahepatic bile duct	10,140	4%
Urinary bladder	13,050	4%	Leukemia	9,680	3%
Non-Hodgkin lymphoma	11,460	4%	Non-Hodgkin lymphoma	8,480	3%
Brain & other nervous system	10,190	3%	Brain & other nervous system	7,830	3%
All sites	321,160		All sites	285,360	

2020, American Cancer Society, Inc., Surveillance Research

Overdiagnosis is harming patients and action is required, says chief medical officer

By **Kate Aubusson**

15 October 2018 – 12:00am

[A](#)[A](#)[A](#)

Australia's chief medical officer has backed moves to protect patients and safeguard the sustainability of the health system against the growing problem of too much medicine.

Overdiagnosis is [exposing healthy people to tests and treatments](#) that are at best useless, and at worst trigger aggressive procedures with devastating side effects, a formidable alliance of peak doctors colleges, researchers, advocates and public health experts warned.



Michael Shirley was diagnosed with prostate cancer and told he needed a radical prostatectomy. Thirteen years after saying no to the surgery he wants men to know they have other options. WOLTER PEETERS

Need for Better Diagnostic, Predictive Tools

Diagnostic: *Identifying presence of disease*

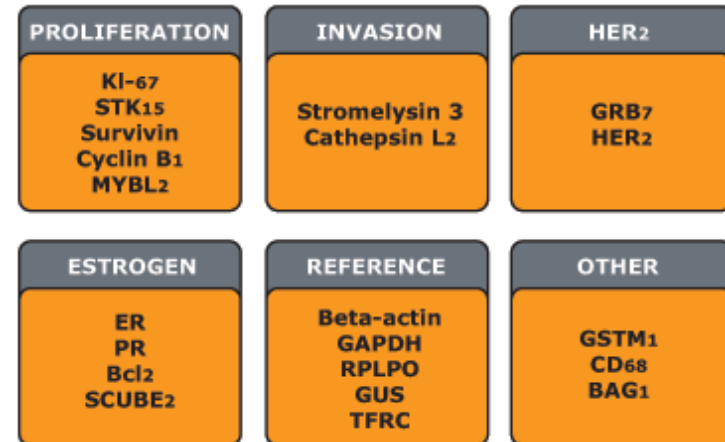
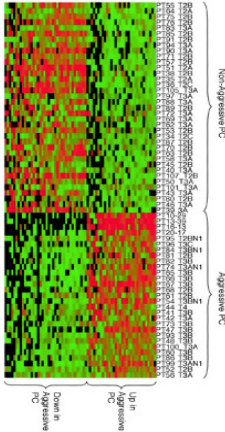
Prognostic: *Predicting Disease Outcome, progression*

Predictive: *Predicting Response to treatment*

Precision Medicine: *Using Prognostic and Predictive Tools for Tailoring Therapy for a given patient based off specific risk profile*

Which cancer patients will receive added benefit from chemotherapy?

Oncotype DX molecular assay (Genomic Health, Inc.)

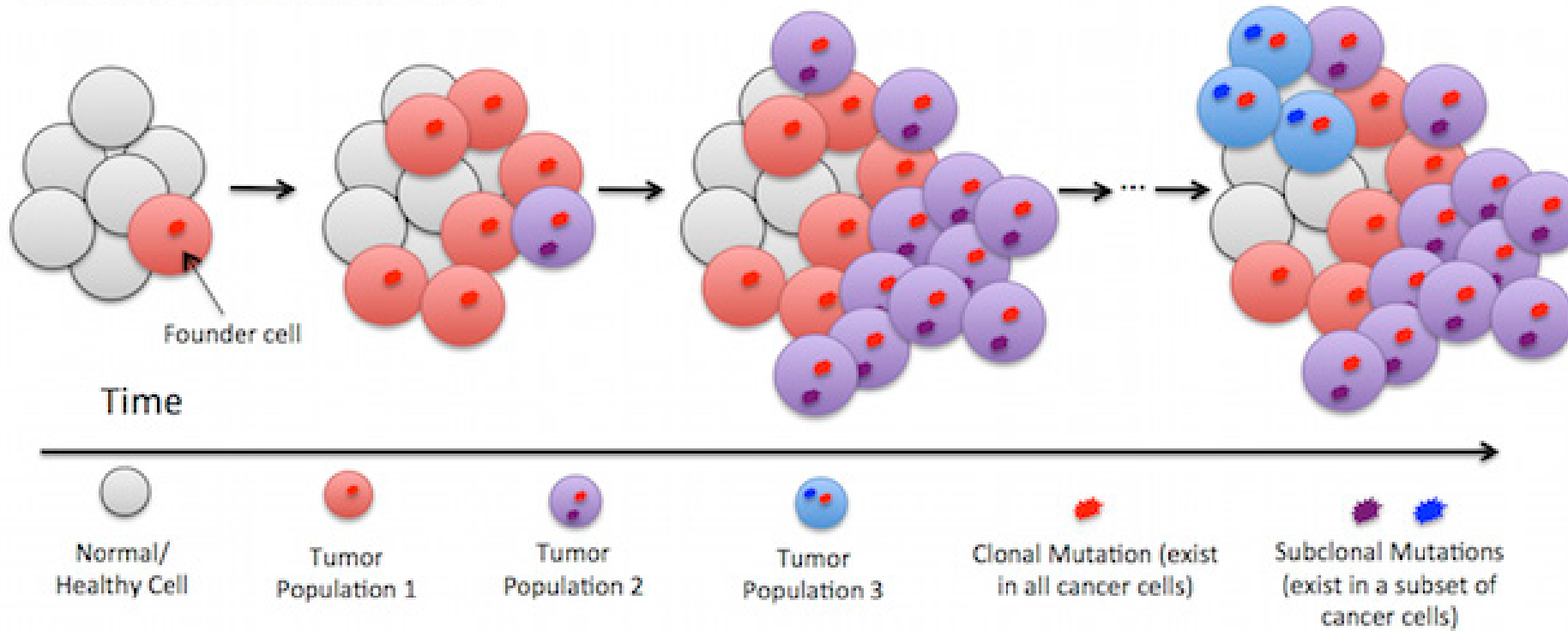


Recurrence Score = **+0.47** x HER2 Group Score
-0.34 x ER Group Score
+1.04 x Proliferation group Score
+0.10 x Invasion Group Score
+0.05 x CD68
-0.08 x GSTM1
-0.07 x BAG1

Paik et al., N Engl J Med 2004 351: 2817-2826

Intra-tumoral heterogeneity

Clonal Theory (Nowell 1976)



PATHOMICS

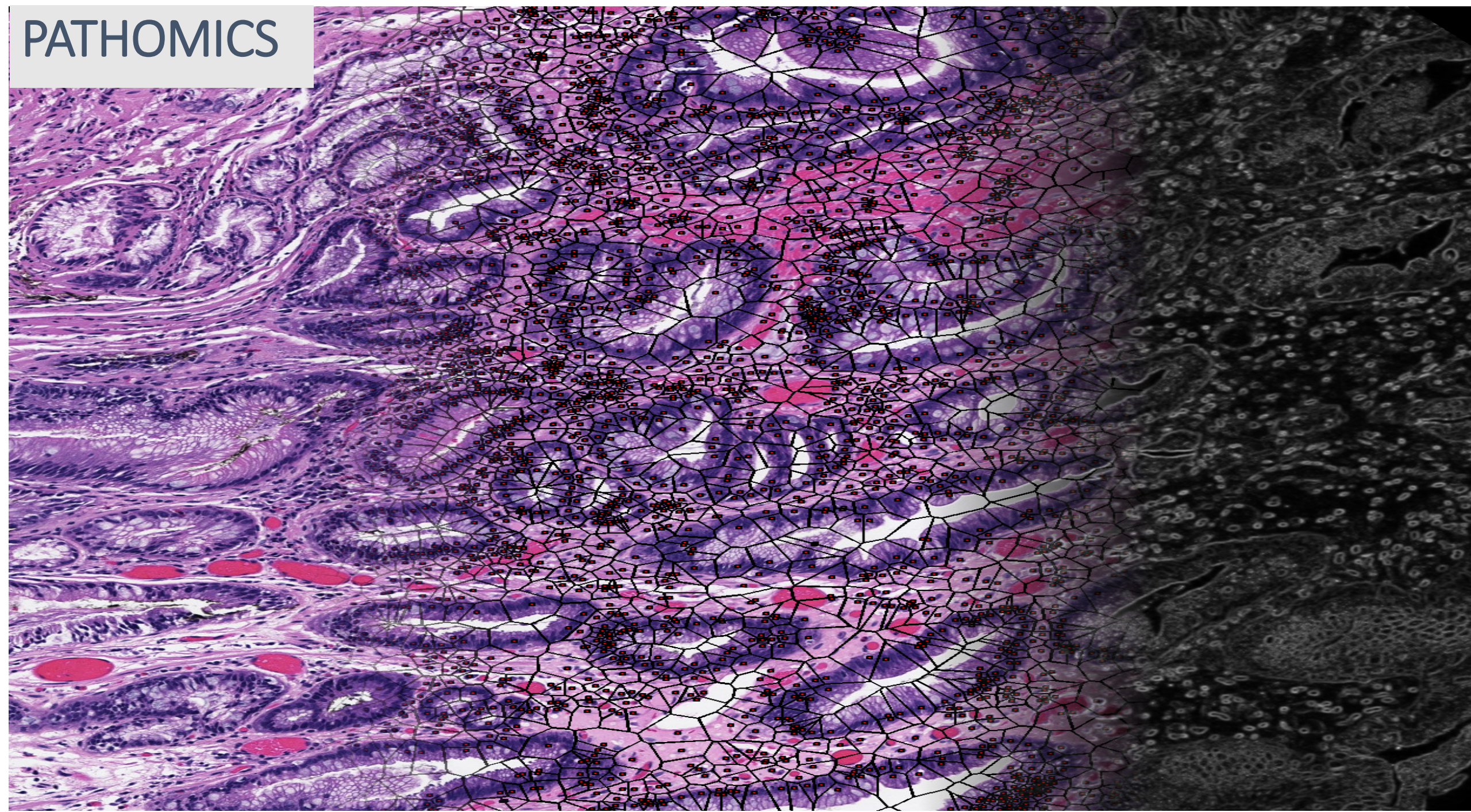
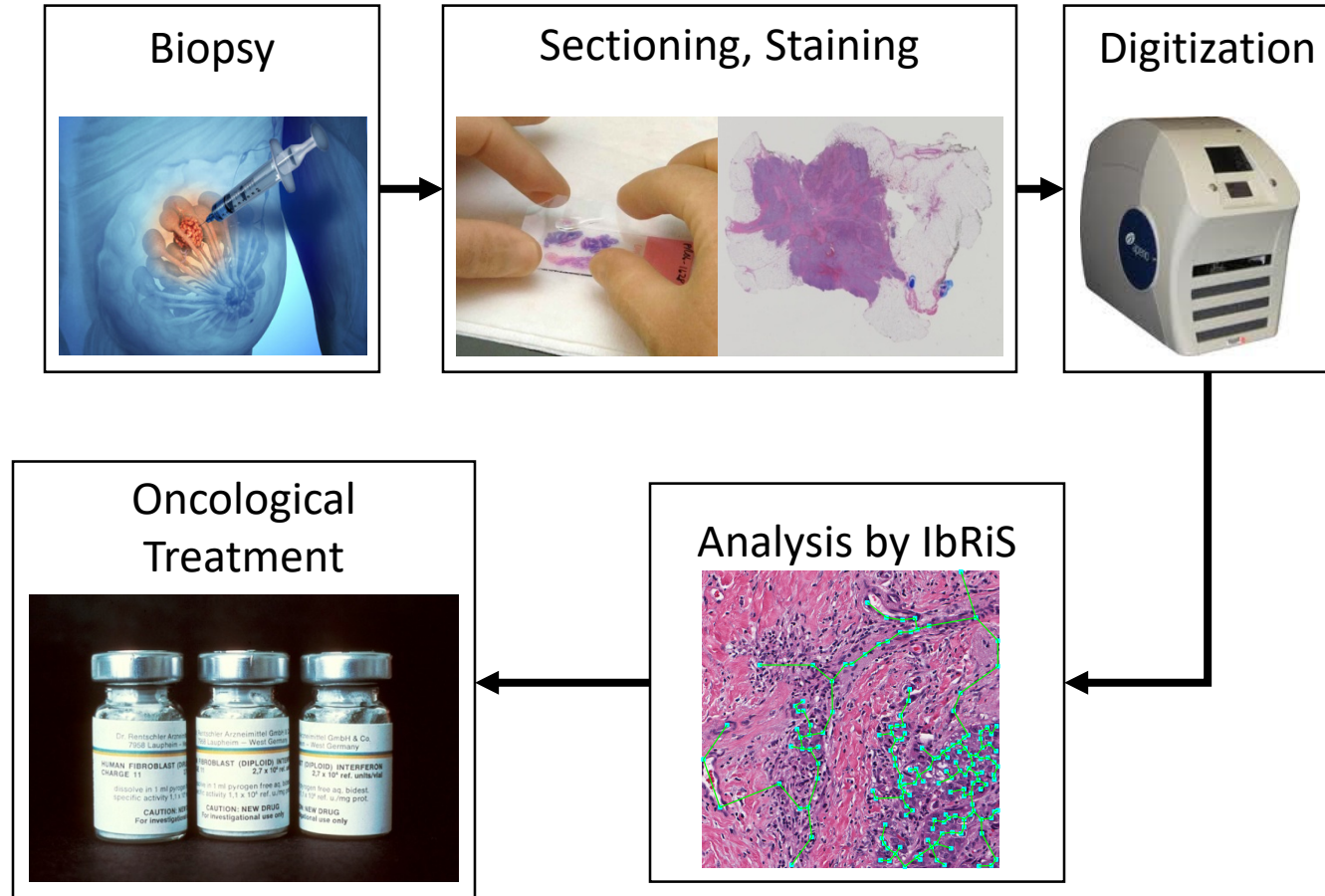
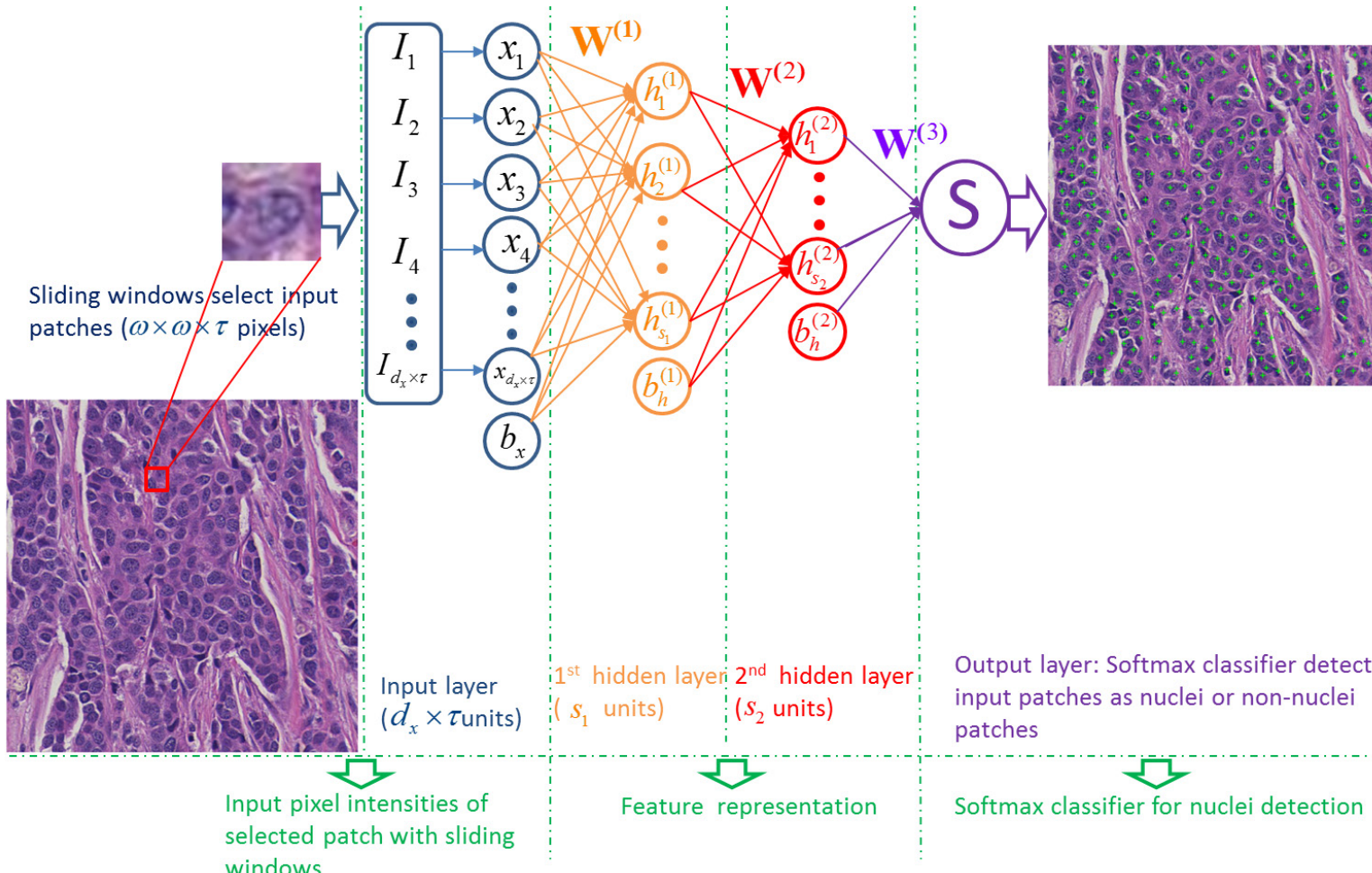


Image-based Risk Score (Ibris)



Stacked Sparse Auto-encoder for Nuclei Detection



Xu J, et al. "Stacked Sparse Autoencoder (SSAE) based Framework for Nuclei Patch Classification on Breast Cancer Histopathology", ISBI2014.

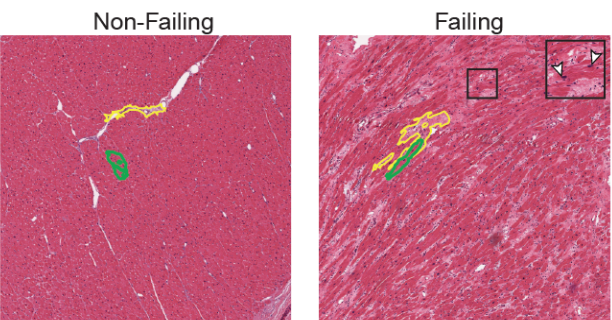
Xu J, et al. "Stacked Sparse Autoencoder (SSAE) for Nuclei Detection on Breast Cancer Histopathology". IEEE Trans. on Medical Imaging, 2015

Zhang X, Dou H, Xu J, Zhang S, "Fusing Heterogeneous Features for the Image-Guided Diagnosis of Intraductal Breast Lesions", IEEE Journal of Biomedical and Health Informatics, 2015

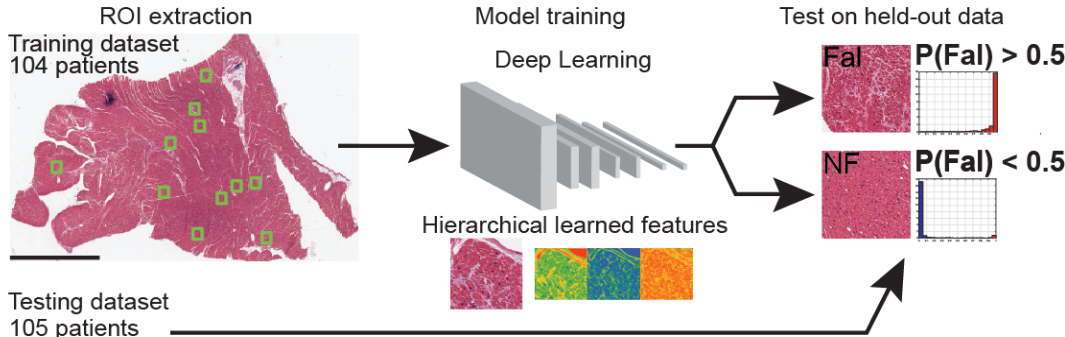
Lu C, Xu H, Xu J, Mandal M, and Madabhushi A, "Multiple Passes Adaptive Voting for Nuclei Detection in Histopathological Images", IEEE Journal of Biomedical and Health Informatics, (Under Preparing)

A deep learning classifier identifies patients with heart failure using WSI of H&E tissue biopsies

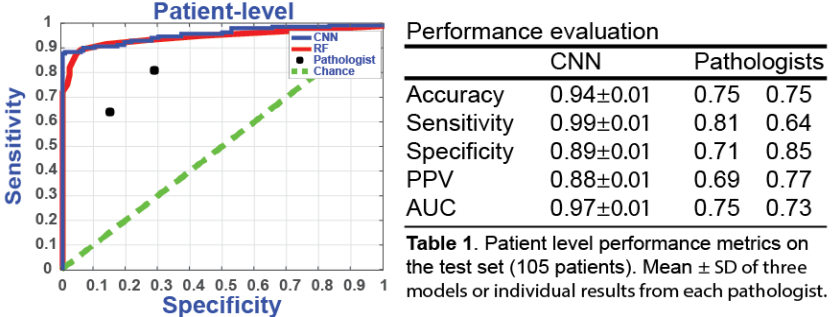
a Cardiac histopathology in heart failure



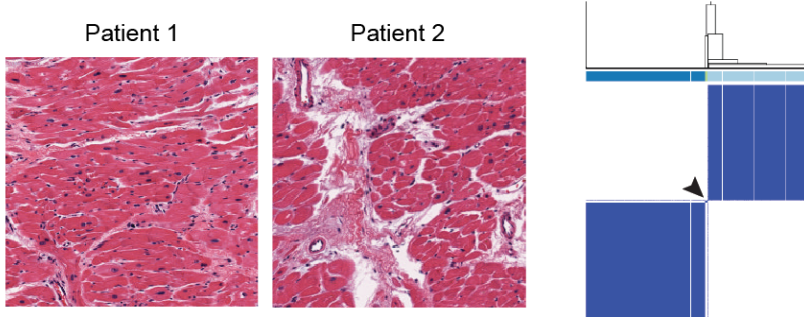
b Training a deep convolutional neural network



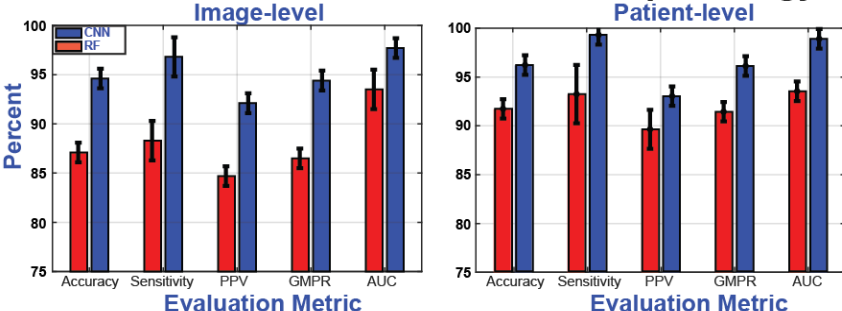
c Detection of clinical heart failure



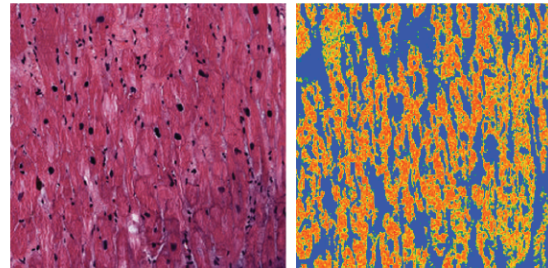
d Algorithms identify tissue pathology in normal patients



e Detection of heart failure or severe pathology



f An example of a feature learned from the CNN



The original H&E stained image is shown on the left. The hidden layer activations for one feature, shown on the right, is strongest in myocyte tissue. Thus, the CNN learned that segmenting myocyte tissue is a useful feature to detect patients with heart failure



CASE SCHOOL
OF ENGINEERING
CASE WESTERN RESERVE
UNIVERSITY



Center for Computational
Imaging and Personalized
Diagnostics



Perelman
School of Medicine
UNIVERSITY OF PENNSYLVANIA

Is there a smarter path to artificial intelligence? Some experts hope so

Originally published June 24, 2018 at 5:00 pm | Updated June 25, 2018 at 12:59 am

But now some scientists are asking whether deep learning is really so deep after all.

In recent conversations, online comments and a few lengthy essays, a growing number of AI experts are warning that the infatuation with deep learning may well breed myopia and overinvestment now — and disillusionment later.

“There is no real intelligence there,” said Michael I. Jordan, a professor at the University of California, Berkeley, and the author of an essay published in April intended to temper the lofty expectations surrounding AI.

“And I think that trusting these brute-force algorithms too much is a faith misplaced.”

More on AI

IBM’s robot debater is ready to convince you that you’re wrong

IBM pits computer against human debaters



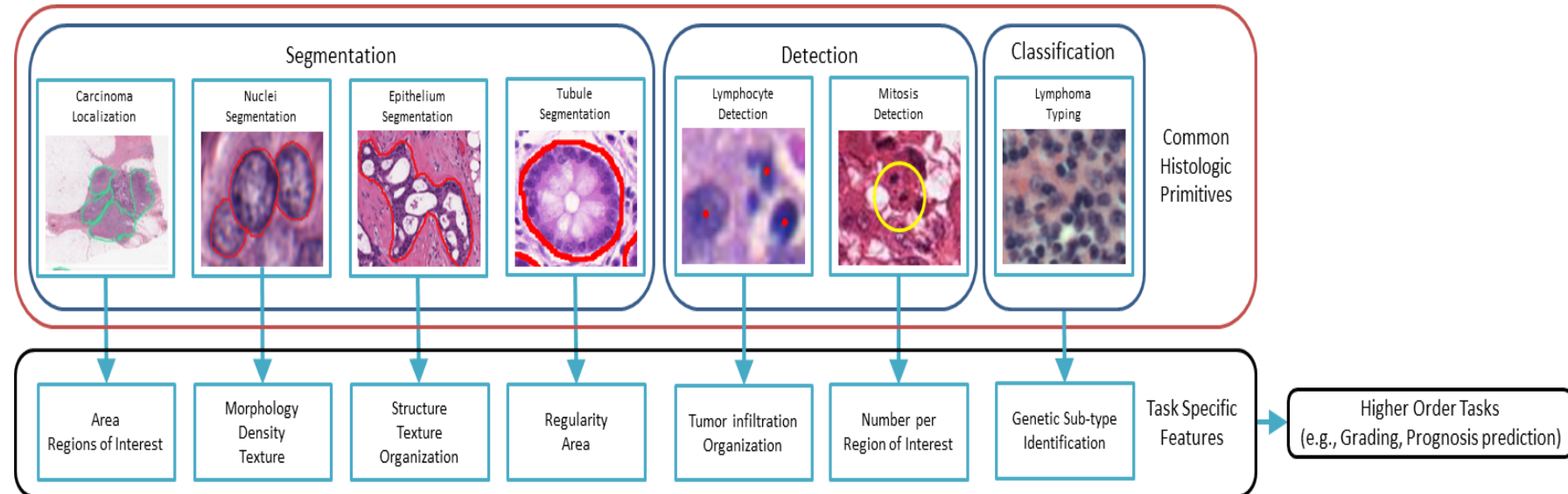
Husky or Wolf? Using a Black Box Learning Model to Avoid Adoption Errors

Past Tides

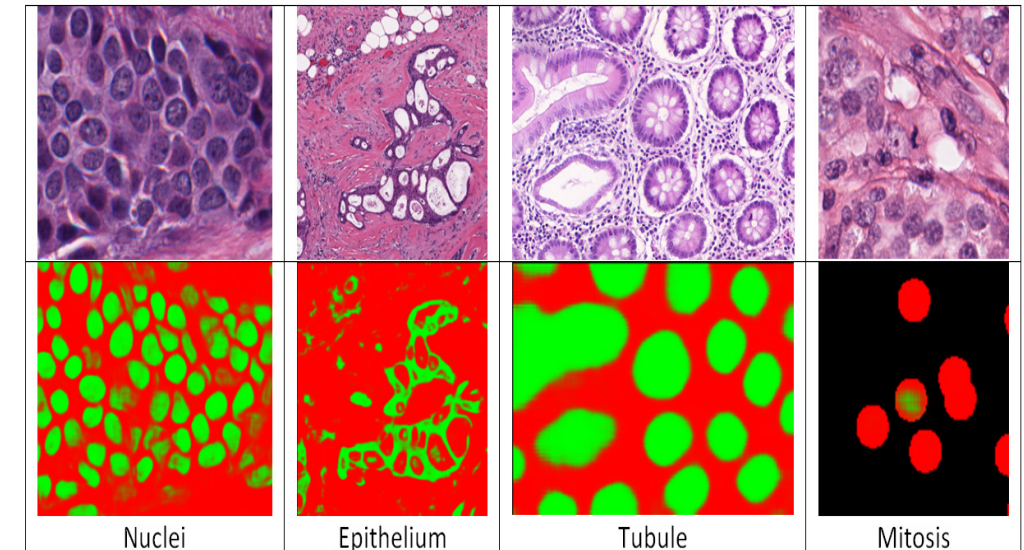
August 24, 2017 By Wendy Wolfson

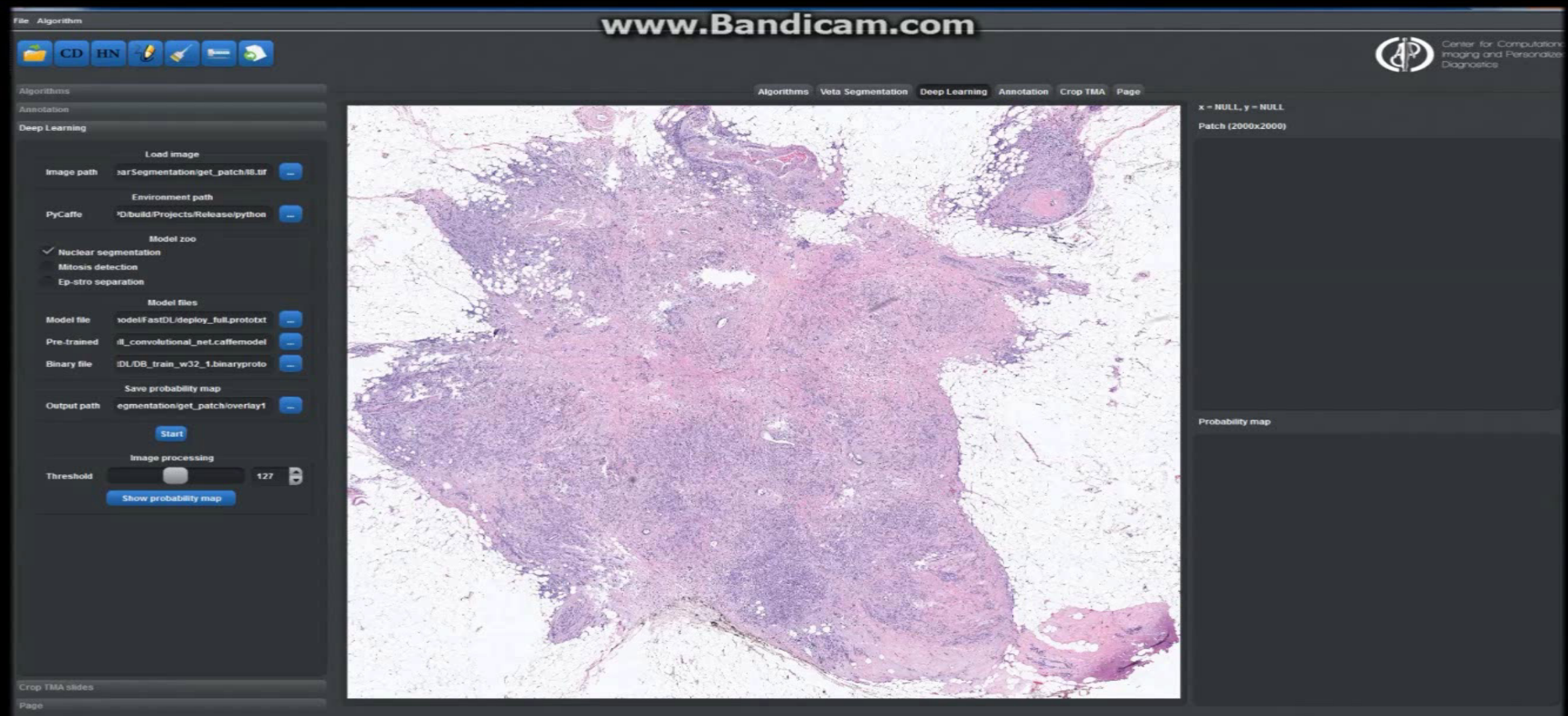
Say you want to adopt a dog, from a picture, and you task your machine learning system to classify the image as either a husky, which would be safe to adopt, or a wolf, which probably is not a good idea. Can you get that photograph classified with certainty? “Because researchers don’t have insights into what is going on they can easily be misled,” said Sameer Singh, assistant professor in the UCI Department of Computer Science. “Classification is core to machine learning,” said Singh, describing ‘black box’ machine learning predictions at the Association for Computing Machinery (ACM) July 12 meeting at the Cove. Machine learning is pervasive in our lives—from email to games. “It’s in our phones,” said Singh, a machine learning and natural language processing expert. “It is in our houses. It is basically everywhere.” One of his students created a wolf/dog classifier in a few hours that seemed to work—at first.

Deep Learning can be extremely useful for segmentation of individual Histologic Primitives and structures

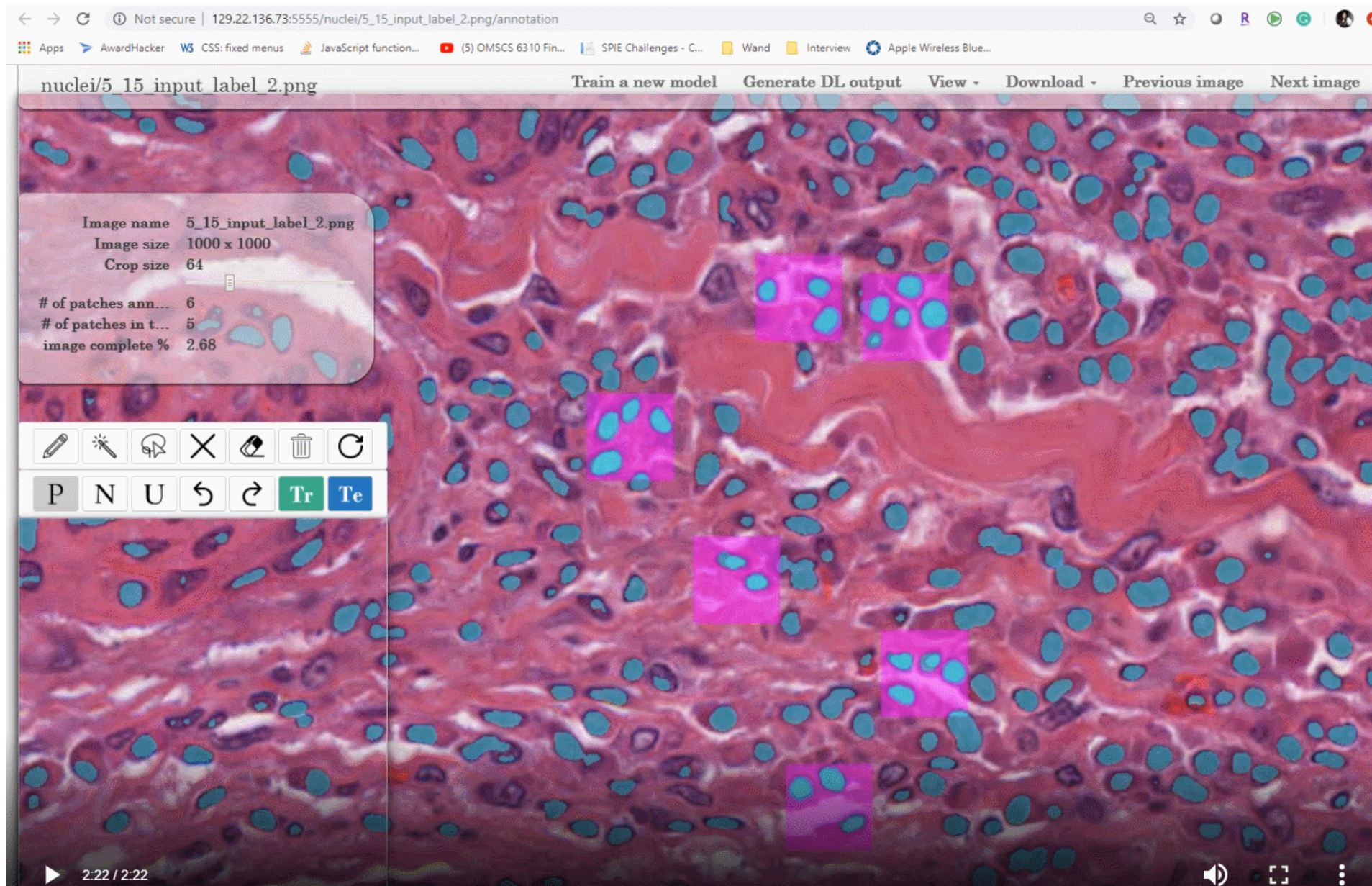


Flowchart of typical workflow for digital pathology research. Histologic primitives (e.g., nuclei, lymphocytes, mitosis, etc.) are identified, after which biologically relevant features are extracted use in downstream applications.

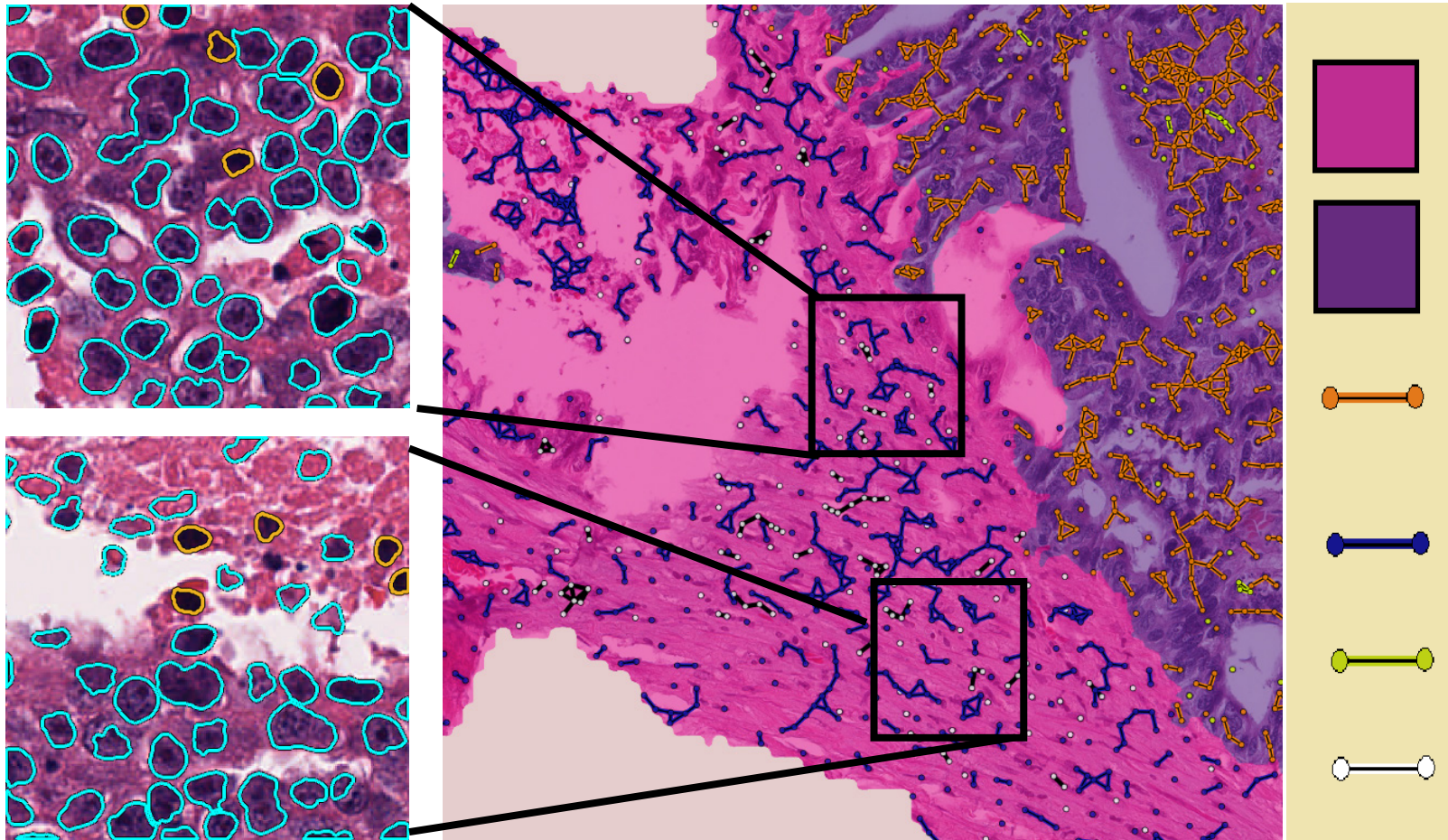




Quick annotator



Nuclei segmentation and sub graph constitution



Stromal region

Epithelial region

Cancer cell clusters

Stromal cell clusters

Tumor infiltrating lymphocytes

Stromal tumor infiltrating lymphocytes

Collagen fiber detection

Epithelium segmentation

Collagen vectors in tumor-associated stroma

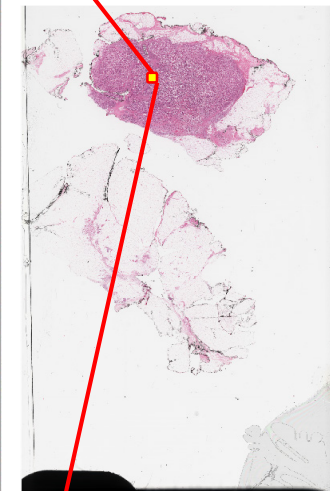
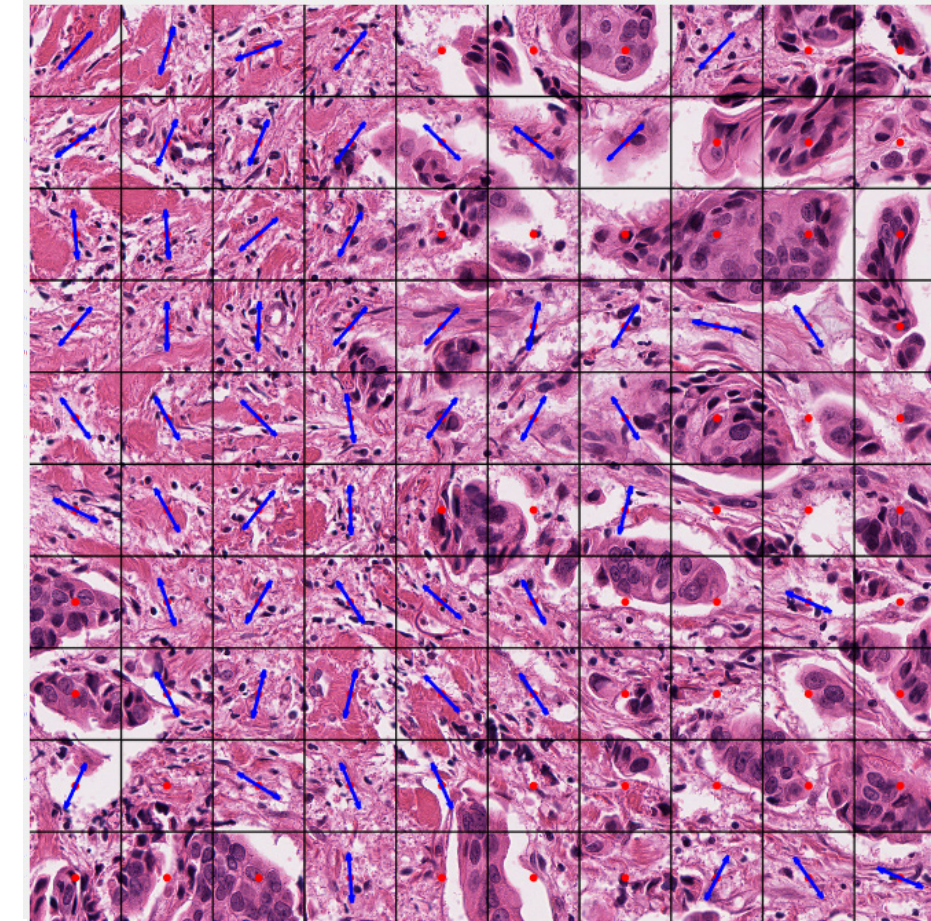
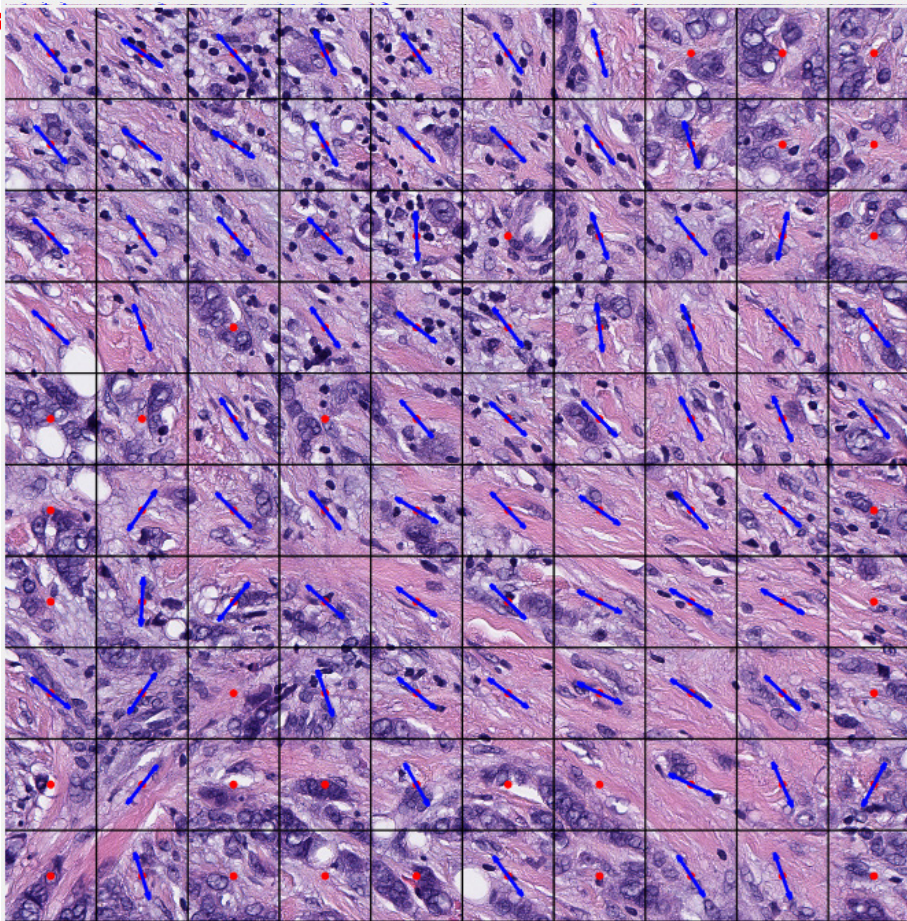
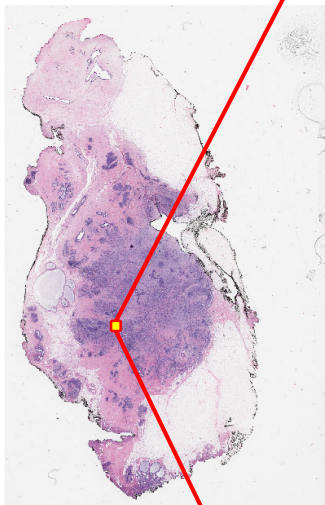
Collagen fiber orientation disorder calculation

Low degree of disorder

High degree of disorder

Short term survival

long term survival



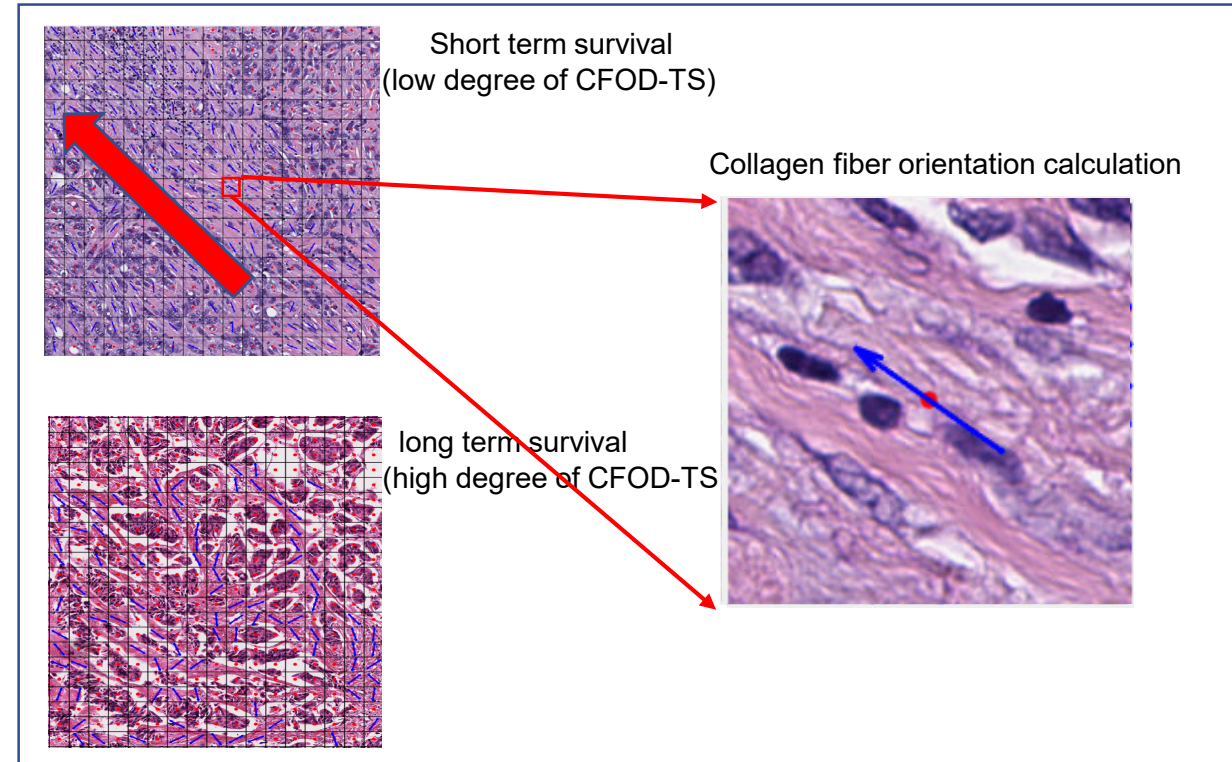
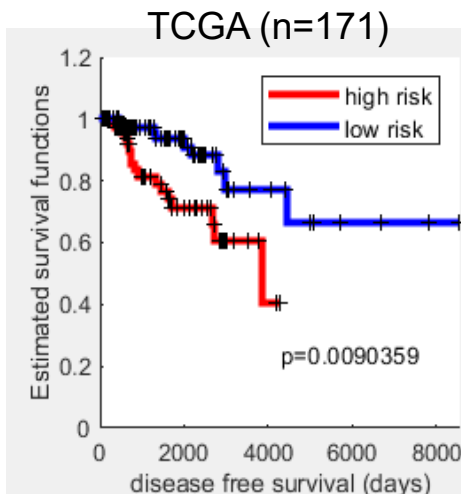
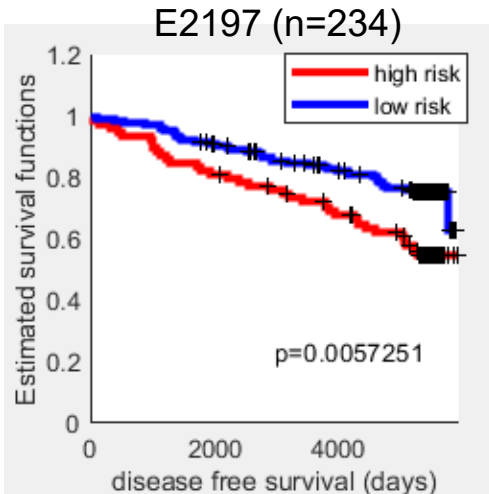
Disorder of collagen fiber orientation associated with risk of recurrence in ER+ breast cancers in ECOG-ACRIN E2197 & TCGA

Unmet Clinical Need

- Early stage ER+ breast cancer (BC) is the most common type of breast cancer in the United States
- Predicting the likelihood of recurrence for patients helps physicians plan more tailored treatment strategy to improve survival rate.

Results:

- Collagen Fiber Orientation Disorder in Tumor associated Stroma (CFOD-TS) was independently prognostic for ER+ BCs in E2197 and TCGA.



Take away:

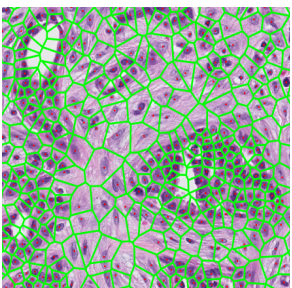
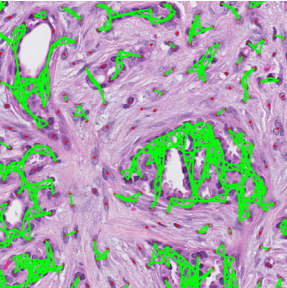
- Over-expression of CFOD-TS was independently associated with lower likelihood of recurrence and could potentially serve as a prognostic marker of outcome for ER+ invasive breast cancer.

Combination of Computer Extracted Features of Nuclear morphology, Tubular Formation, and Mitotic Count from H&E Images Predict Disease Free Survival in Estrogen Receptor Positive (ER+) Breast Cancer

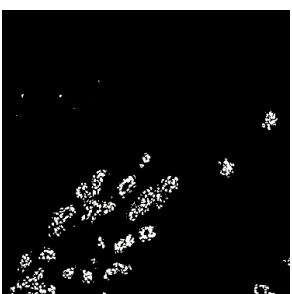
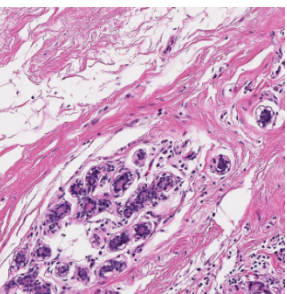
Background

- ER+ breast cancer (BCa) is the most common type of breast cancer in the United States
- Nottingham combined histologic grade reflects how far the tumor architecture and cytology deviate from normal, and how rapidly the tumor proliferates.

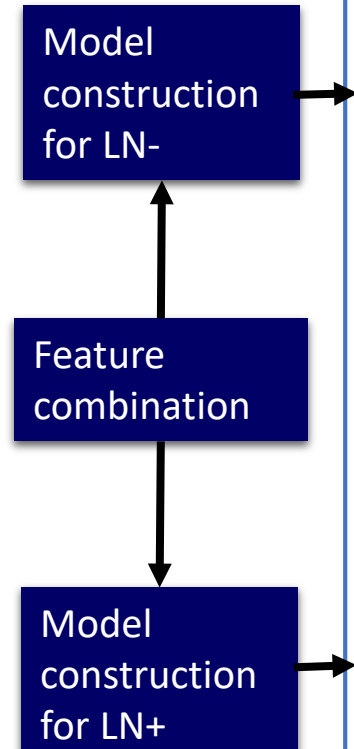
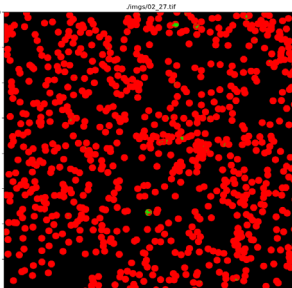
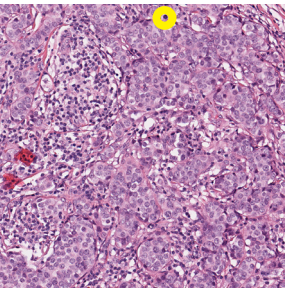
Nuclear morphology



Tubule formation

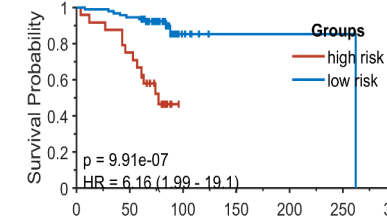


Mitotic count



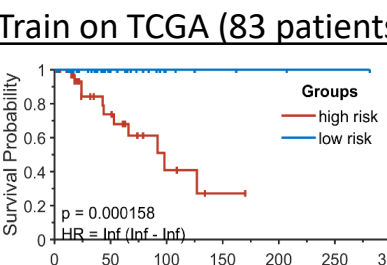
Results

■ LN- Train on UH (116 patients)



	high risk	18	0	0	0	0	C
	low risk	92	87	6	1	1	C

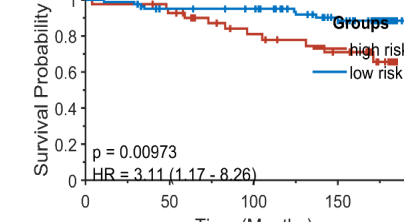
■ LN+ Train on TCGA (83 patients)



	high risk	41	14	4	1	0	0	0
	low risk	42	18	5	3	2	1	0

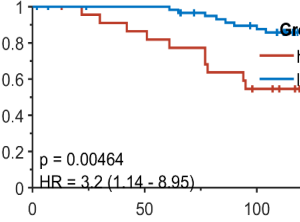
Independent validation on 2 sites

ECOG2197 (121 patients)



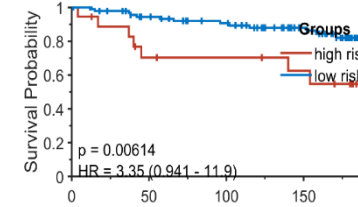
	high risk	41	37	26	20	0	high risk
	low risk	80	72	68	51	0	low risk

Tata (85 patients)



	high risk	23	19	11	0	0	high risk
	low risk	61	58	49	0	0	low risk

UH (11 patients)



	high risk	18	11	10	8	0	high risk
	low risk	94	80	69	49	0	low risk

Takeaway

The combination of nuclear, tubule, and mitotic features is prognostic of disease-free survival (DFS) for the ER+ breast cancer patients.

A Head-to-Head Comparison

	Oncotype DX	IbRiS
Cost of test:	\$4,600	\$4.60
Waiting for results:	2 weeks	20 minutes
Tissue specimen:	Destroyed	Digitized
Accessibility:	USA only	Worldwide

An inexpensive, fast, reliable, accessible prognostic breast cancer test:

PRICELESS

For everything else... there's Mastercard



Combining IbRIS+Oncotype DX: ECOG2197

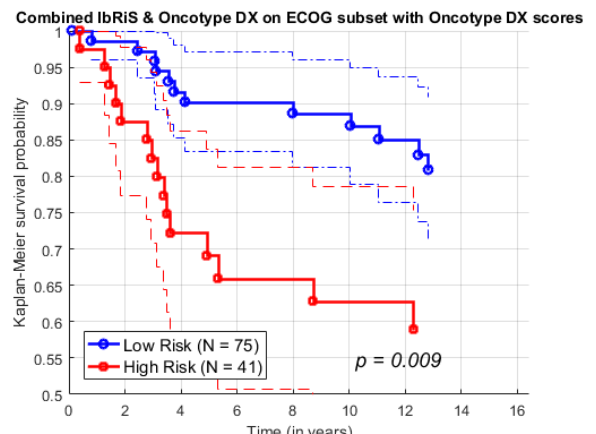
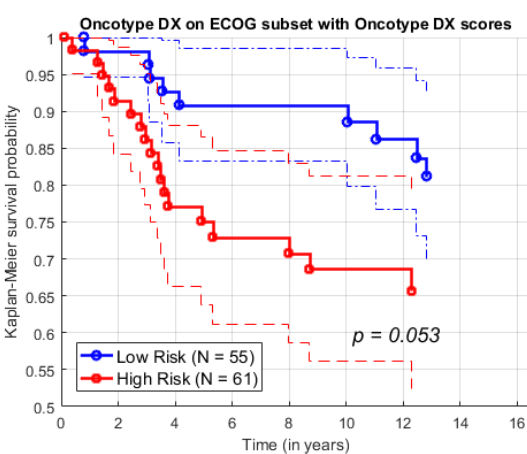
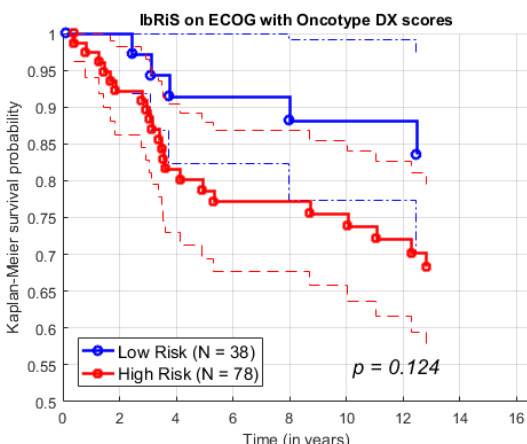
- 378 ER+ breast cancer patients (60 recurrences)
- Node positive, negative axillary lymph nodes, primary tumors at least 1.1 cm
- Endocrine therapy plus chemotherapy
- 116 with Oncotype DX (ODx) scores (27 recurrences)

Assay	% of patients with no recurrence after 10 years classified as low-risk	10-year recurrence rate in low-risk group	% of HER2- patients with no recurrence after 10 years classified as low-risk	10-year recurrence rate in low-risk HER2- group
IbRIS	35.34%	10.87%	37.11%	10.0%

IbRIS performance over all 378 cases

Assay	% of patients with no recurrence after 10 years classified as low-risk	10-year recurrence rate in low-risk group	% of HER2- patients with no recurrence after 10 years classified as low-risk	10-year recurrence rate in low-risk HER2- group
IbRIS	37.5%	17.2%	50.0%	13.3%
ODx	56.3%	20.0%	53.8%	26.3%
IbRIS + ODx	75.0%	20.0%	84.6%	21.4%

Comparison of IbRIS to Onctotype DX over 116 cases with ODx scores



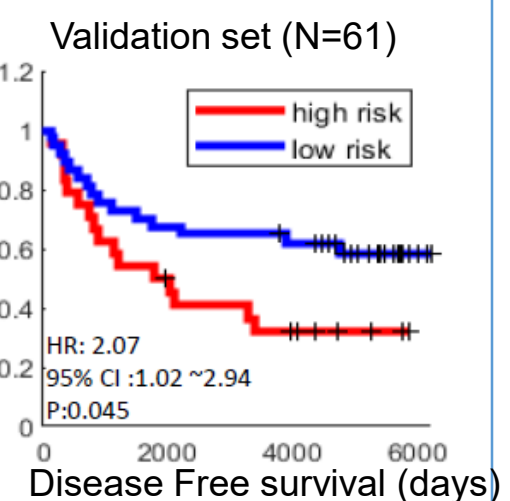
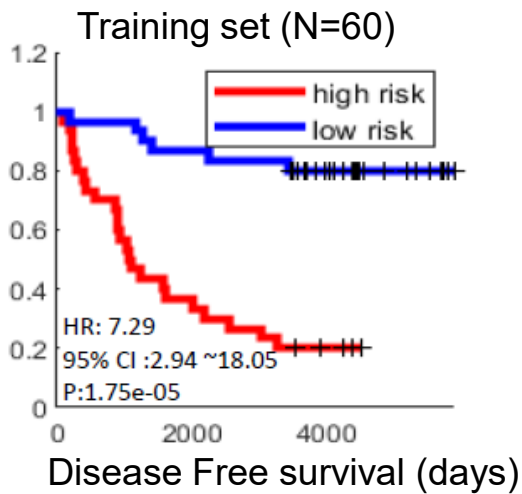
Computer extracted features of nuclear shape, orientation disorder and texture from H&E Whole slide images are associated with disease-free survival in Ductal Carcinoma in situ (DCIS)

Unmet Clinical Need

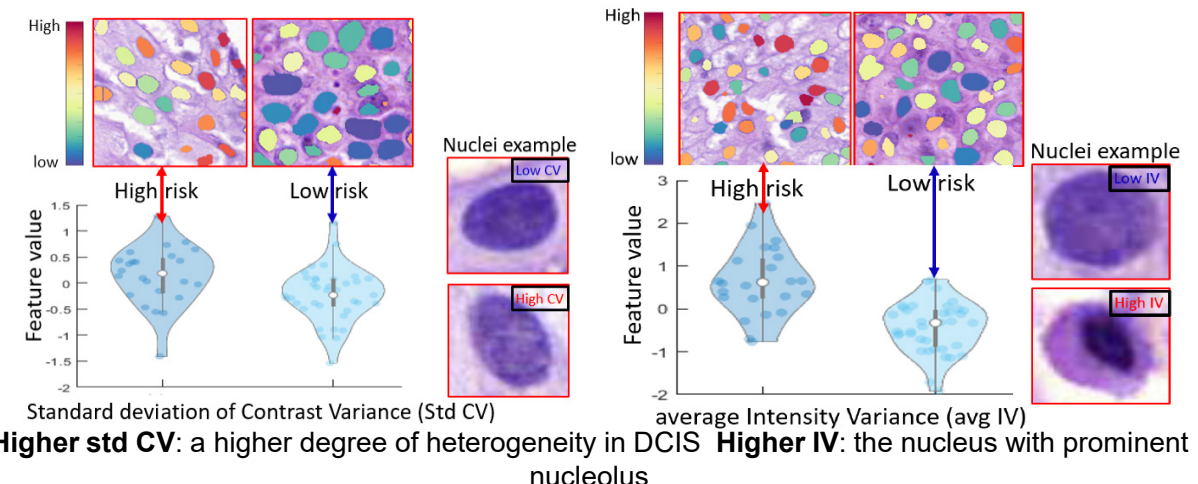
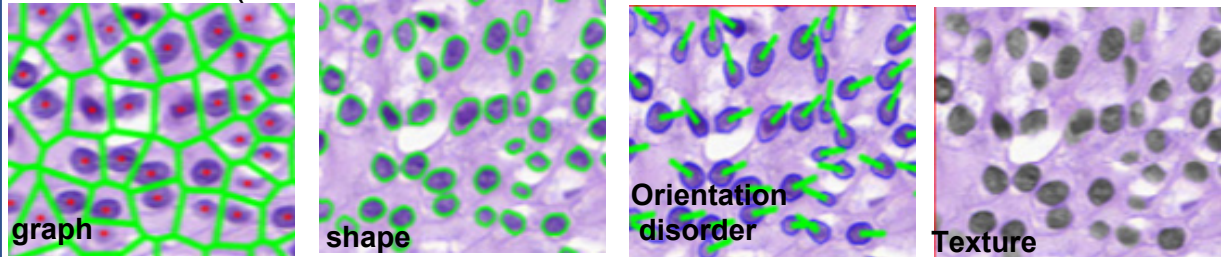
- Gold standard treatment: lumpectomy + adjuvant radiation.
- Identify patients with low-risk DCIS, for whom radiotherapy can often be omitted.
- Gene assays such as Oncotype DX: expensive, time-consuming and tissue destructive.

Results

The Cox regression model built with nuclear morphologic features is prognostic of DCIS



Computationally derived morphometric features in histological (resection) images to assess recurrence risk.

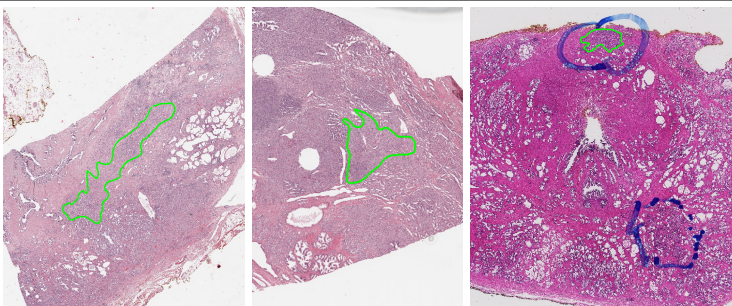


Take Away: Combination of the quantitative nuclear histomorphometric features pertaining to nuclear shape, orientation disorder and Haralick textures is prognostic for DCIS.

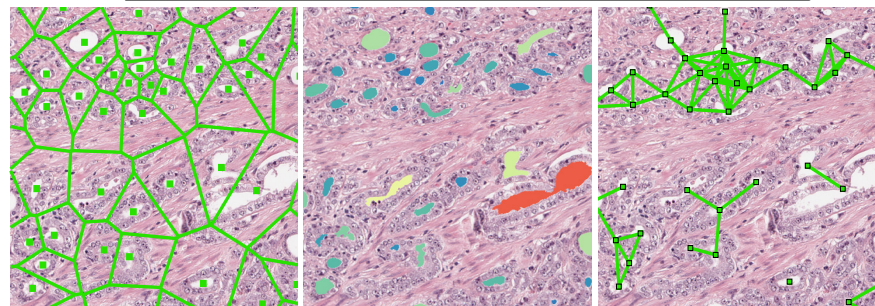


Predicting post-surgical recurrence in prostate cancer

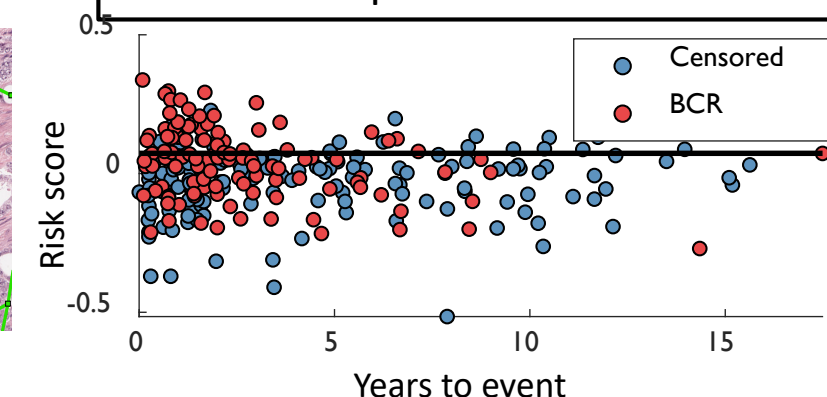
N=907 diagnostic slides from 6 sites



→ Extract 216 gland lumen features

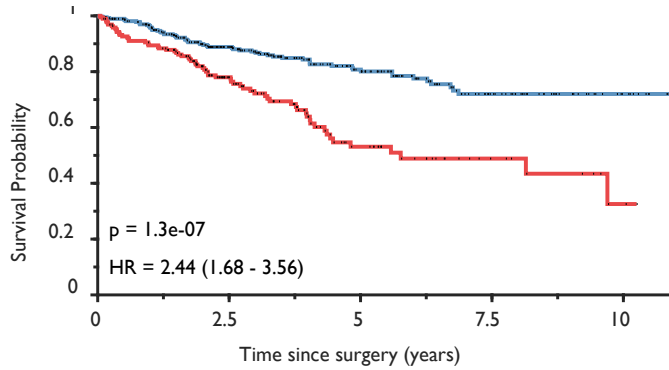


→ Train on 263 patients from one site

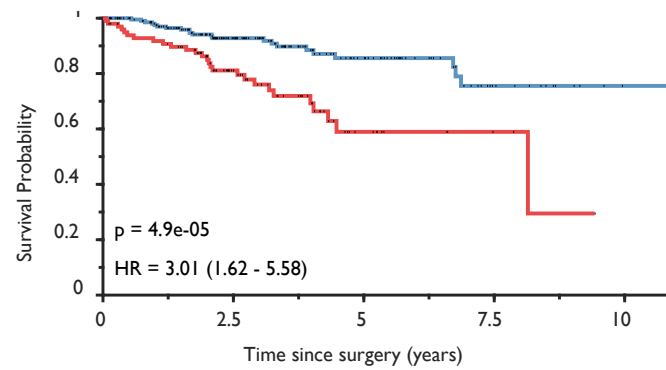


Results

Prognostic in independent validation



Added value in margin-negative patients



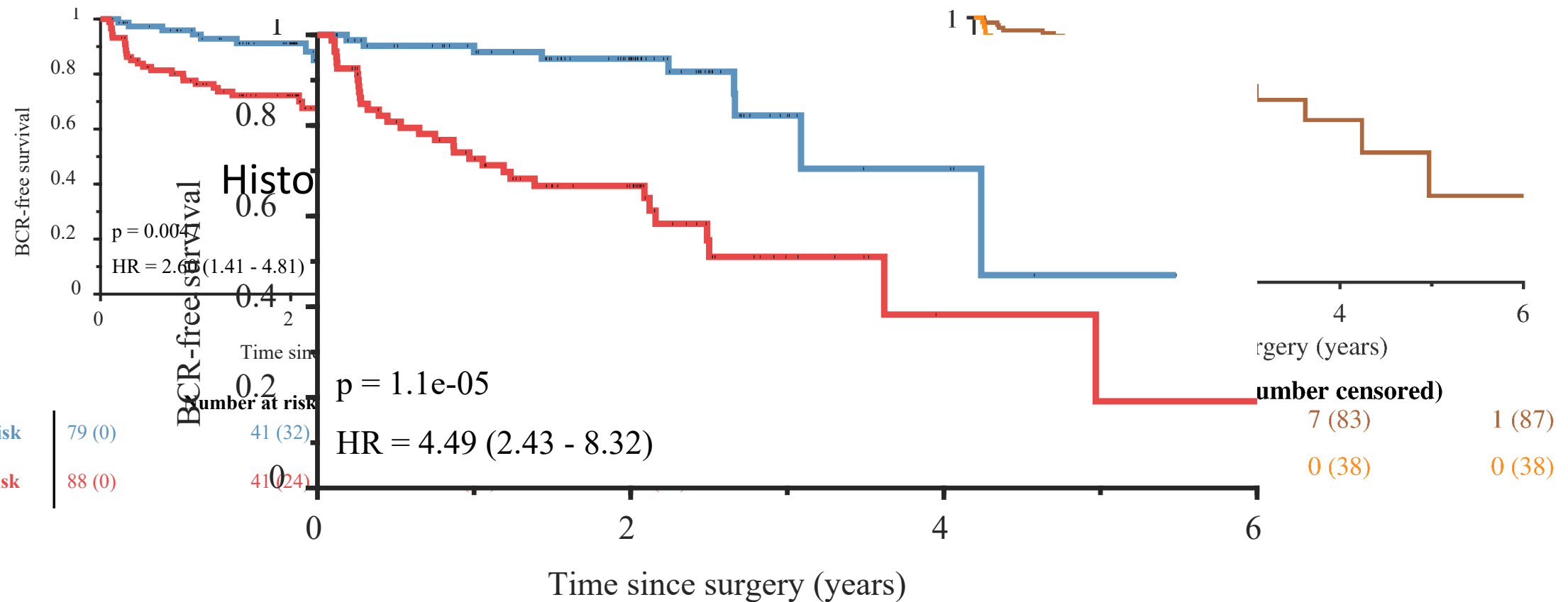
Independent from clinical markers

Covariate	p	HR
Risk score (per 0.1 increase)	<.01	1.33
Grade group >2	<.01	3.05
Positive margins	<.01	2.21
Log2 pre-op PSA	0.24	1.13
Stage >T2a	0.63	1.42

Number at risk (number censored)				
Low-risk	381 (0)	229 (115)	121 (207)	48 (271)
High-risk	193 (0)	99 (55)	33 (98)	11 (118)

Number at risk (number censored)				
Low-risk	224 (0)	118 (93)	51 (154)	15 (187)
High-risk	100 (0)	51 (32)	11 (63)	3 (71)

Image based risk score versus Decipher: Head to Head Comparison



Number at risk (number censored)

Low-risk

86 (0)

47 (35)

5 (73)

0 (77)

High-risk

81 (0)

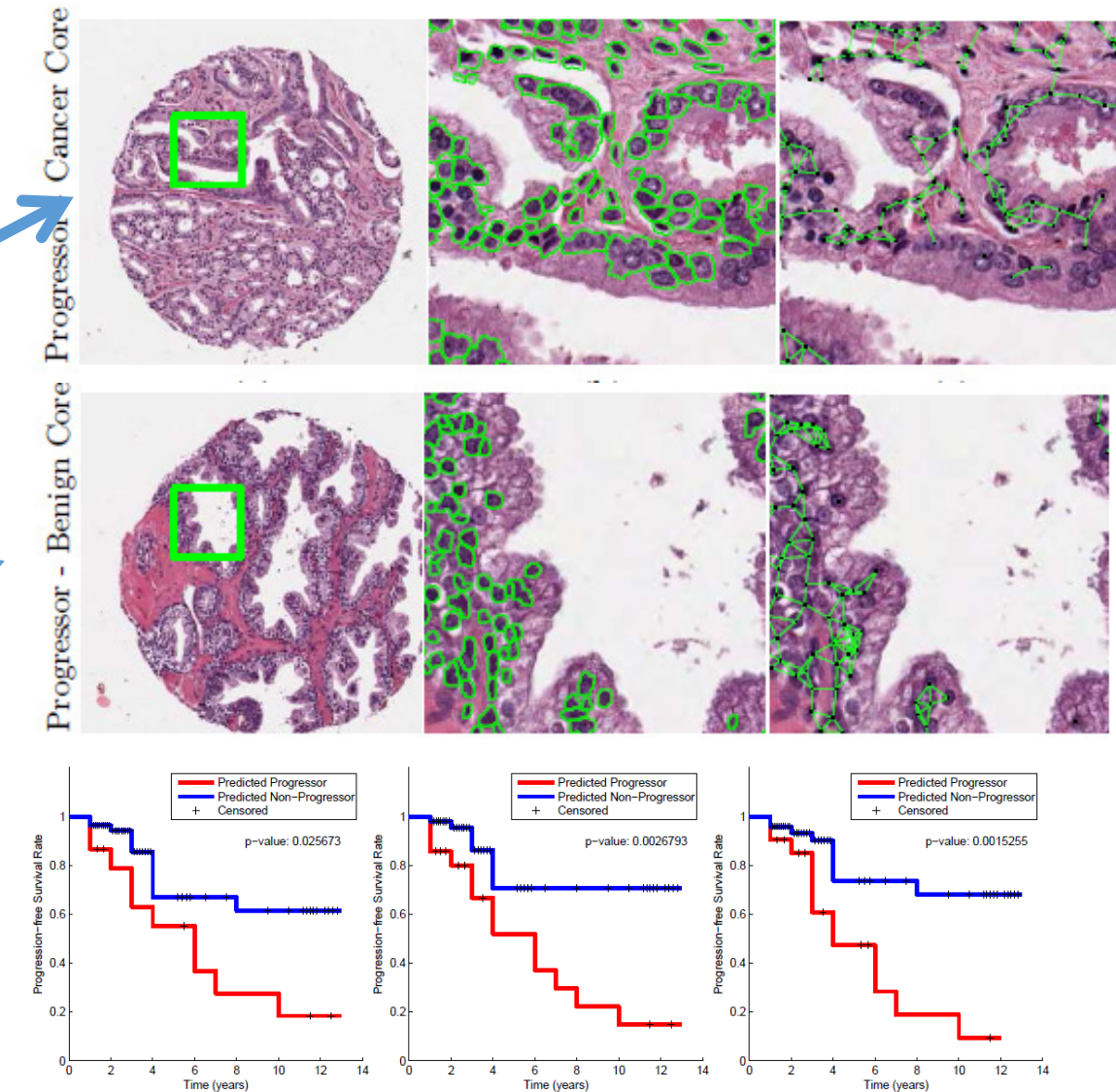
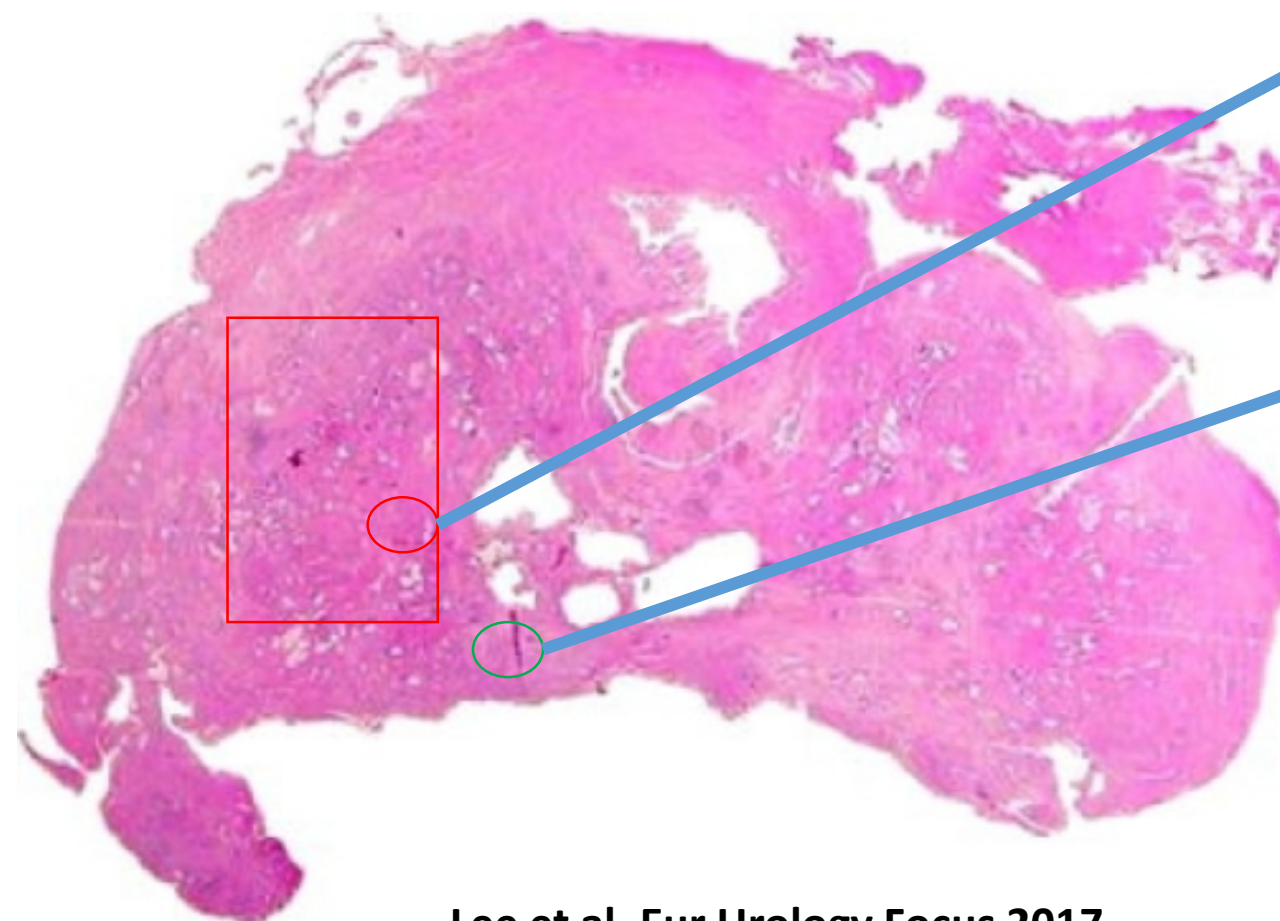
35 (21)

2 (48)

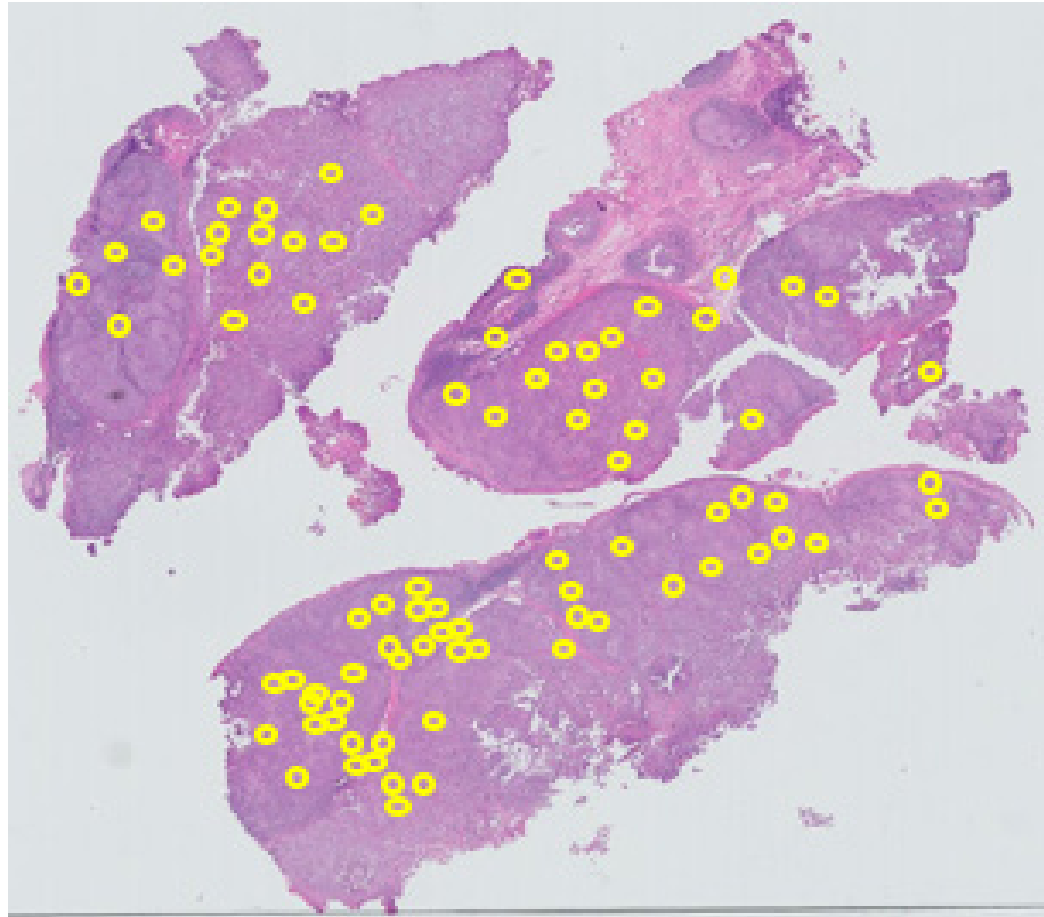
1 (48)

Features from benign regions on surgical specimens of the prostate predict likelihood of cancer recurrence after surgery

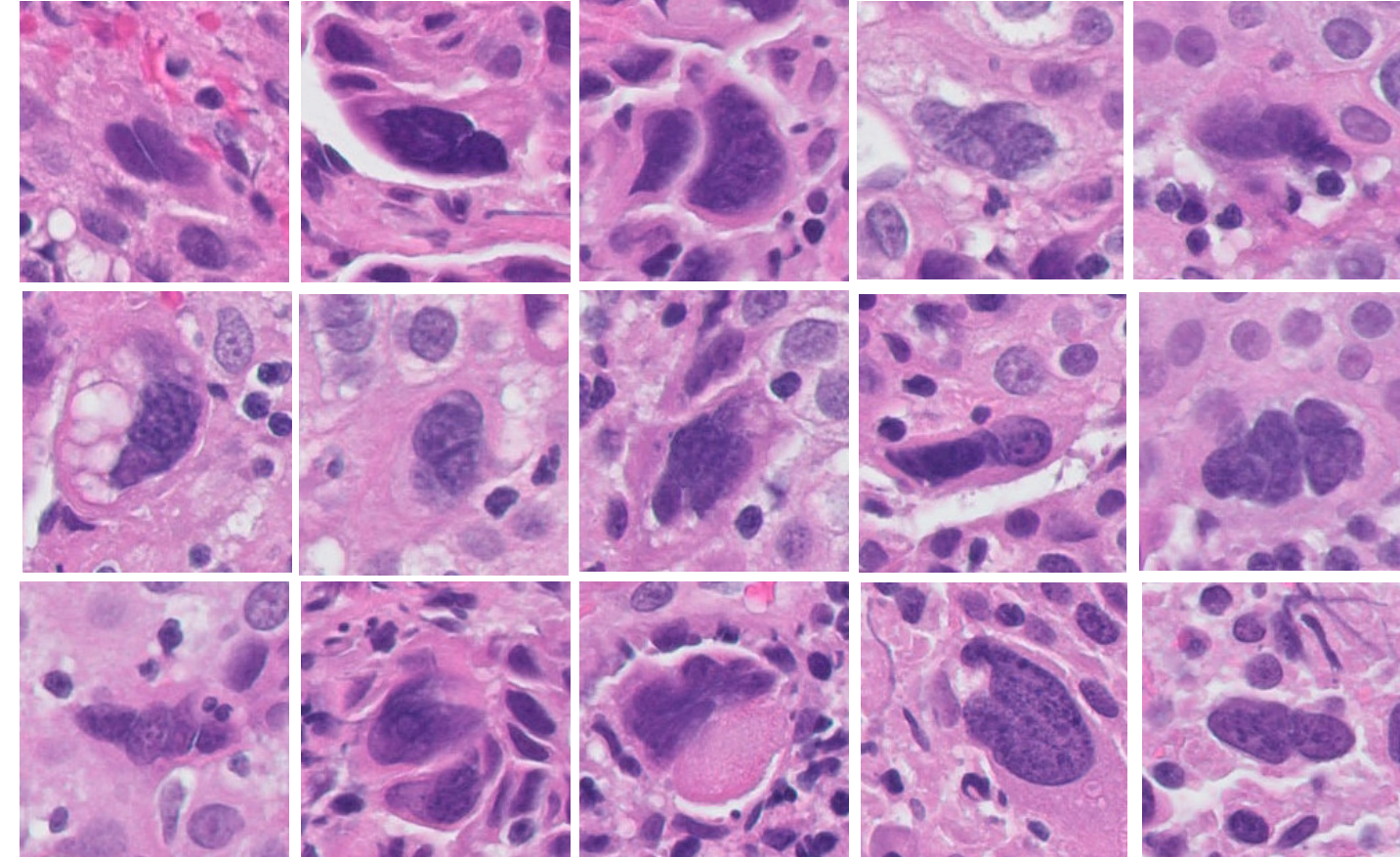
- Field effect provides clues on cancer progression
- Tumor + Adjacent Benign Signature (TABS) outperforms prediction from cancerous regions alone



Computerized Quantitation of Tumor Cell Multinucleation is Strongly Prognostic for p16-Positive Oropharyngeal Squamous Cell Carcinoma

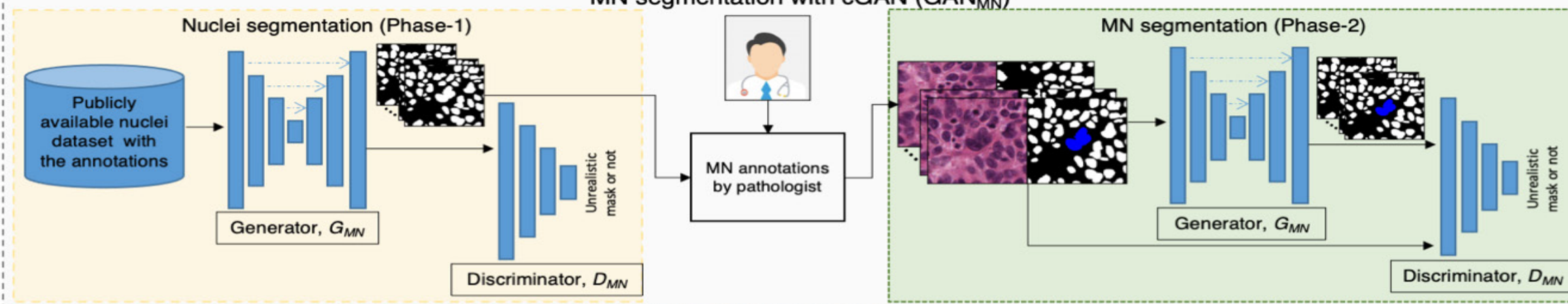


Yellow spots indicates the locations of multinucleation

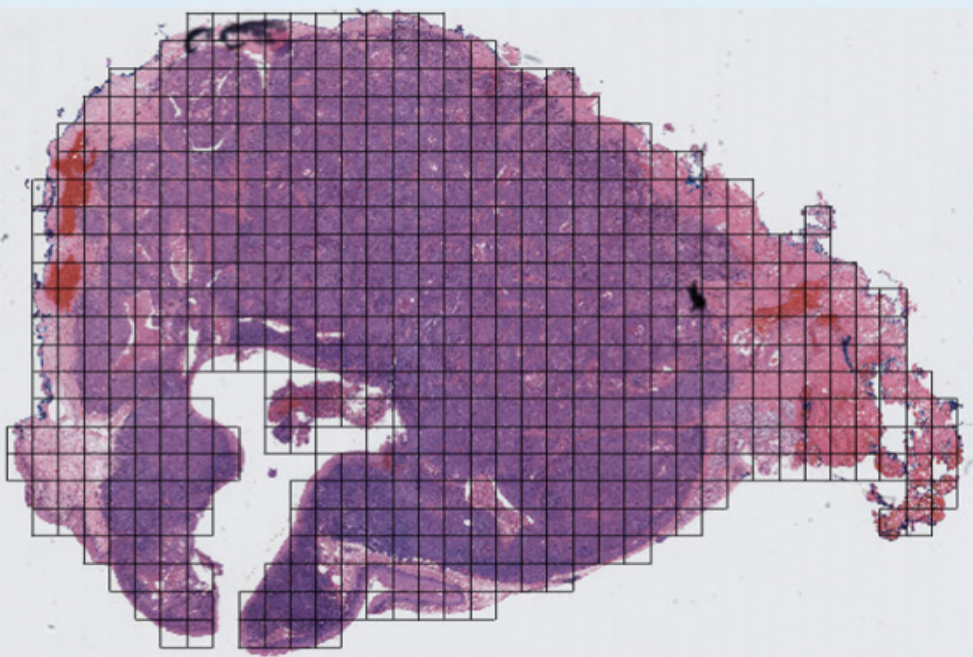


Zoomed in Multinucleation figures

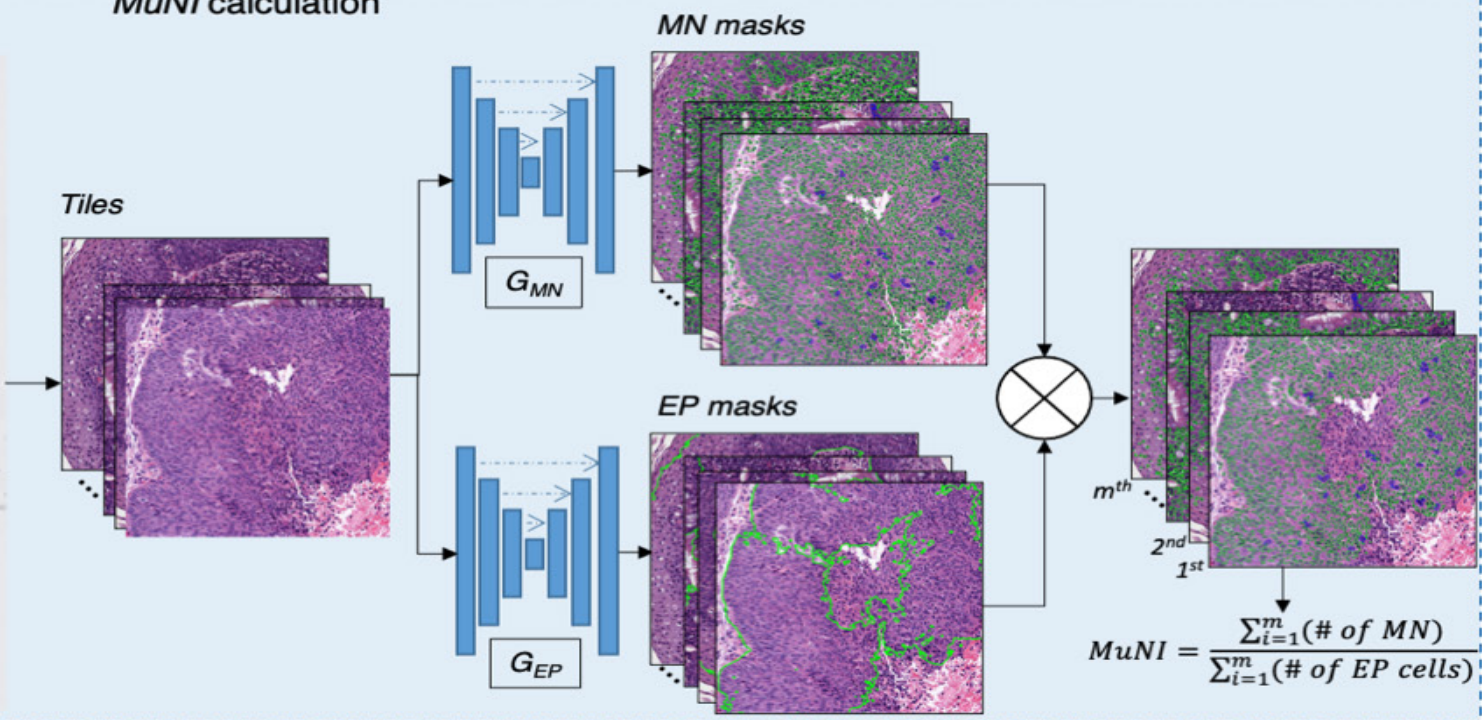
MN segmentation with cGAN (GAN_{MN})



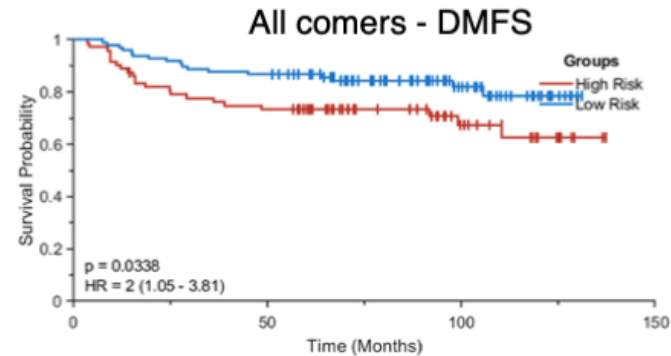
Tiling at 40x



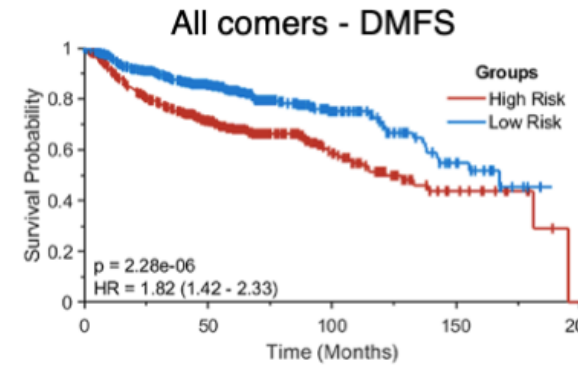
MuNI calculation



Training set

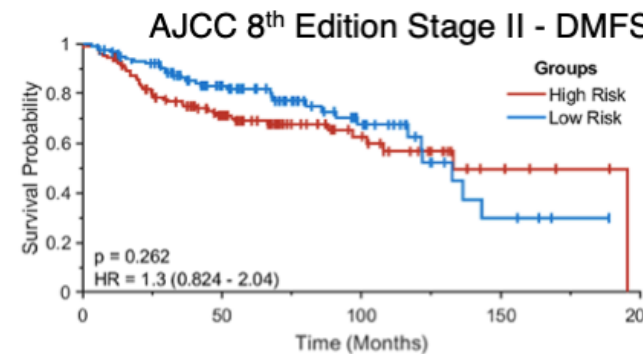


High Risk	72	52	19	0
Low Risk	98	85	32	0

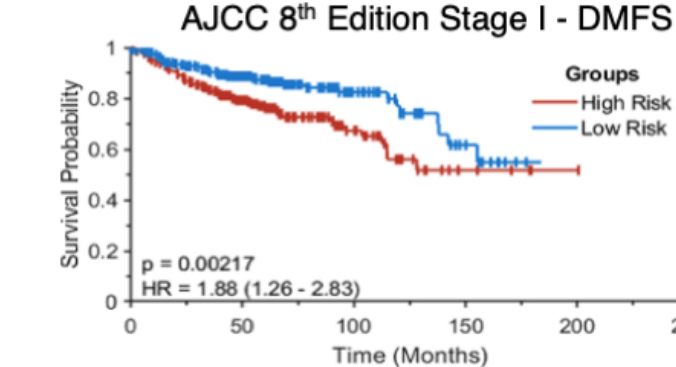


High Risk	484	238	70	13	1
Low Risk	440	253	81	21	0

High Risk	228	118	34	5	1	0
Low Risk	243	140	41	11	0	0



High Risk	128	71	23	5	0
Low Risk	117	68	23	4	0



High Risk	102	49	13	3	0
Low Risk	68	43	17	6	0

High Risk	102	49	13	3	0
Low Risk	68	43	17	6	0

KM-DMFS curves for patients in training/validation cohorts for different cancer stage groups according to AJCC 8th edition definition.

Computerized tumor multinucleation index (MuNI) is prognostic in p16+ oropharyngeal carcinoma: A multi-site validation study

Can F. Koyuncu,¹ Cheng Lu,¹ Kaustav Bera,¹ Zelin Zhang,² Jun Xu,² Paula Andrea Toro Castaño,¹ Germán Corredor,¹ Deborah Chute,³ Pingfu Fu,⁴ Wade L. Thorstad,⁵ Farhoud Faraji,⁶ Justin A. Bishop,⁷ Mitra Mehrad,⁸ Patricia D. Castro,⁹ Andrew G. Sikora,¹⁰ Lester D. R. Thompson,¹¹ R. D. Chernock,¹² Krystle A. Lang Kuhs,¹³ Jingqin Luo,¹⁴ Vlad C. Sandulache,¹⁰ David J. Adelstein,¹⁵ Shlomo Koyfman,¹⁶ James S. Lewis Jr.,¹⁷ and Anant Madabhushi¹

Published March 2, 2021 - [More info](#)

[View PDF](#) 

▲ Abstract

BACKGROUND. p16 positive oropharyngeal squamous cell carcinoma (OPSCC) patients are potentially cured with definitive treatment. However, there are currently no reliable biomarkers of treatment failure in p16 positive OPSCC. Pathologist-based visual assessment of tumor cell multinucleation has been shown to be independently prognostic of disease-free survival in p16 positive OPSCC. However, its quantification is time-intensive, subjective, and at risk of interobserver variability.

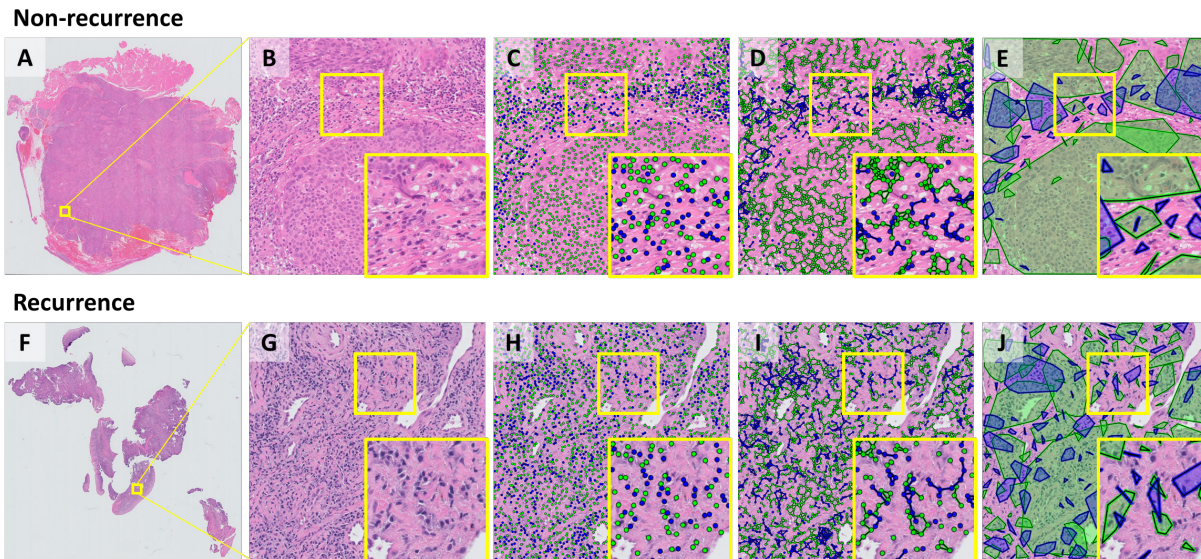
METHODS. We present a deep learning-based metric, the multi-nucleation index (MuNI), for prognostication in p16 positive OPSCC. This approach quantifies tumor multi-nucleation from digitally scanned hematoxylin eosin (H&E)-stained slides. Representative H&E whole slide images from 1,094 previously untreated p16 positive OPSCC patients were acquired from six institutions for optimizing and validating MuNI.

RESULTS. MuNI was prognostic for disease-free (DFS), overall (OS), or distant metastasis-free (DMFS) survival in p16 positive OPSCC with HRs of 1.78(95%CI:1.37-2.30), 1.94(1.44-2.60), and 1.88(1.43-2.47), respectively, independent of age, smoking status, treatment type, and T/N-categories in multivariable analyses. It was also prognostic for DFS, OS, and DMFS in OPSCC patients at stages I and III.

CONCLUSION. MuNI holds promise as a low-cost, tissue non-destructive, H&E stain based digital biomarker test for counseling, treatment, and surveillance of p16 positive OPSCC patients. These data support further confirmation of MuNI in prospective trials.

FUNDING. This work was supported by the National Cancer Institute of the National Institutes of Health (under award numbers 1U24CA199374-01, R01CA202752-01A, R01CA208236-01A1, R01CA216579-01A1, R01CA220581-01A1, 1U01CA239055-01), the National Institute for Biomedical Imaging and Bioengineering (1R43EB028736-01), the National Center for Research Resources (1C06RR12463-01), the VA Merit Review Award (IBX004121A) from the United States Department of Veterans Affairs Biomedical Laboratory Research and Development Service, the DoD Breast Cancer Research Program Breakthrough Level 1 Award (W81XWH-19-1-0668), the DOD Prostate Cancer Idea Development Award (W81XWH-15-1-0558), the DOD Lung Cancer

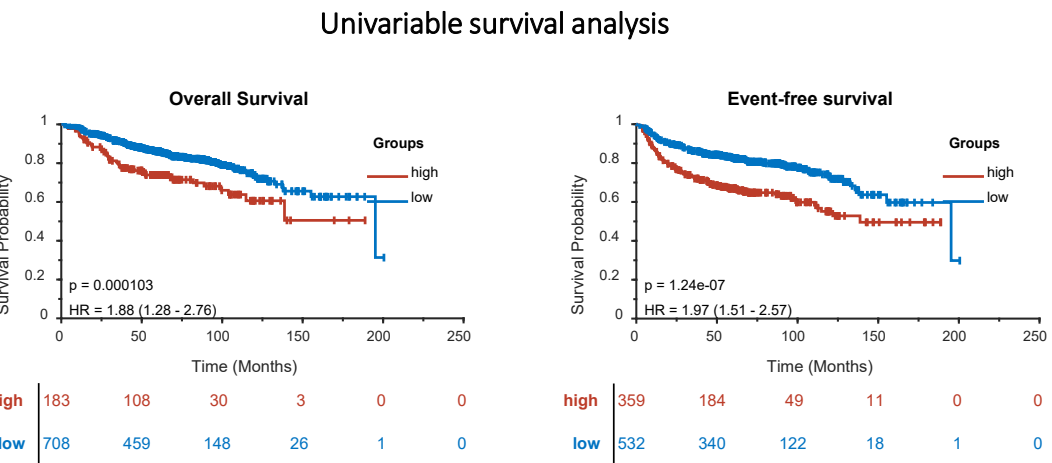
Predicting prognosis in Head and Neck Cancers by characterizing the interplay between TILs and surrounding cancer cells



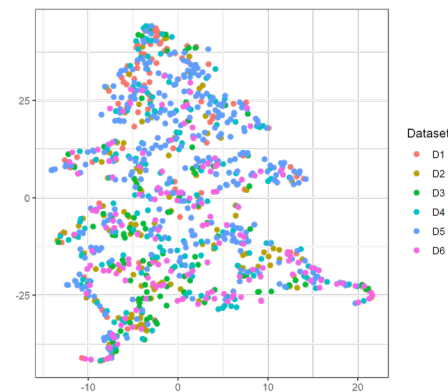
Datasets	# Cases	# Recurrences	# Deaths
Houston VA (D1)	94	30	61
JHU (D2)	121	33	13
WU (D3)	107	16	21
Kaiser (D4)	169	30	37
CCF (D5)	336	55	74
VUMC (D6)	158	17	29
Total	985	181	235

Feature discovery
and model training

Independent validation



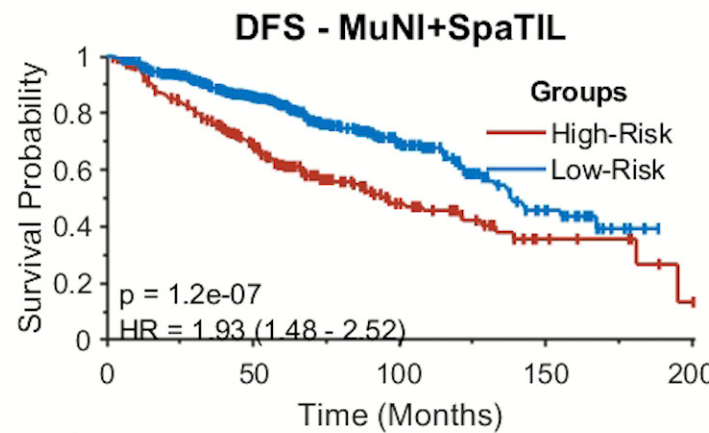
Unsuperv. Clustering of Features



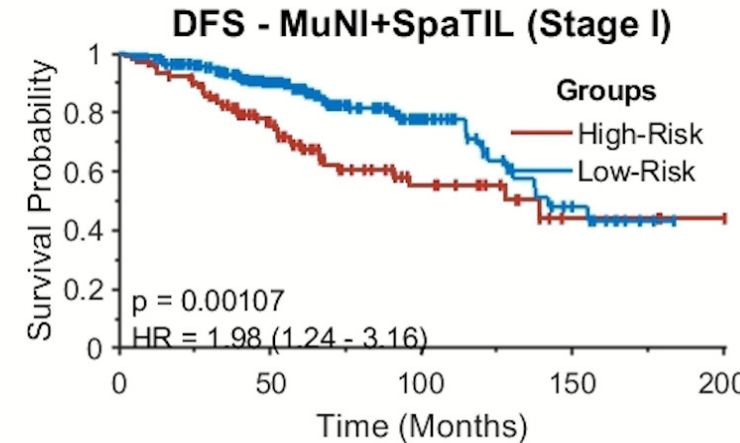
Multivariable survival analysis

Variable	Overall Survival		Event-free Survival	
	p-value	HR (CI)	p-value	HR (CI)
Age	8.04E-07	1.05(1.03-1.07)	1.00E-05	1.04 (1.02-1.05)
Race	0.3385	0.73(0.39-1.38)	0.1919	0.68 (0.38-1.21)
Sex	0.624	0.88(0.53-1.47)	0.793	1.06 (0.67-1.69)
Smoking	0.0176	1.56(1.08-2.24)	0.198	1.22 (0.90-1.64)
Overall st.	0.1389	0.74(0.49-1.10)	0.0331	0.68 (0.47-0.97)
T-stage	0.0012	1.60(1.21-2.13)	0.0001	1.68 (1.31-2.16)
N-stage	0.0126	1.42(1.08-1.86)	0.0017	1.47 (1.16-1.87)
OP-TIL	0.008	1.60(1.13-2.26)	0.0001	1.74 (1.32-2.28)

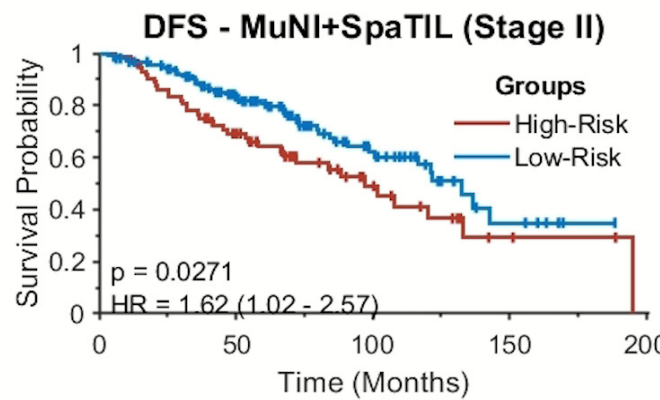
Combining biomarkers results in even better prognosis – even within individual stage groups



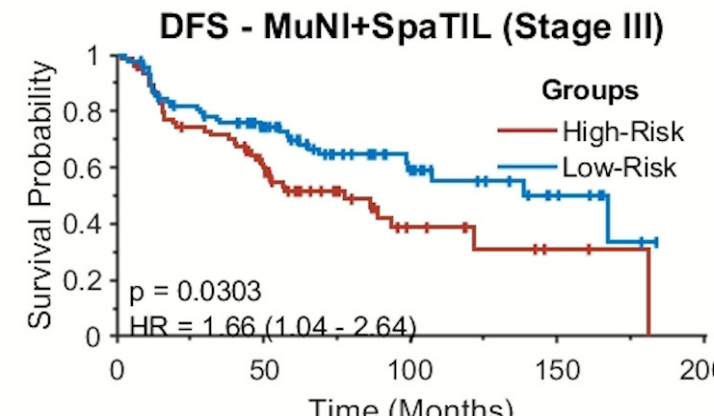
	267	146	43	8	1
High-Risk	267	146	43	8	1
Low-Risk	532	323	101	24	0



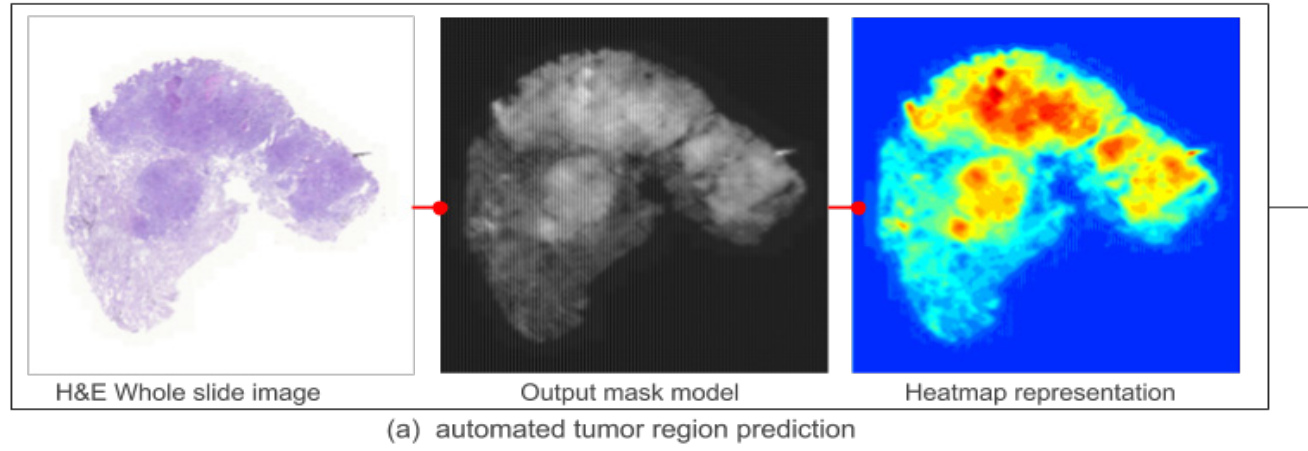
	106	61	20	3	1
High-Risk	106	61	20	3	1
Low-Risk	286	173	49	11	0



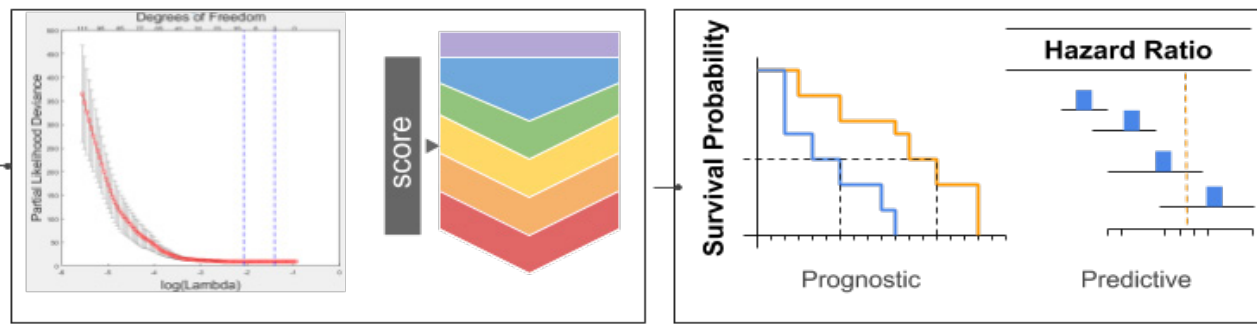
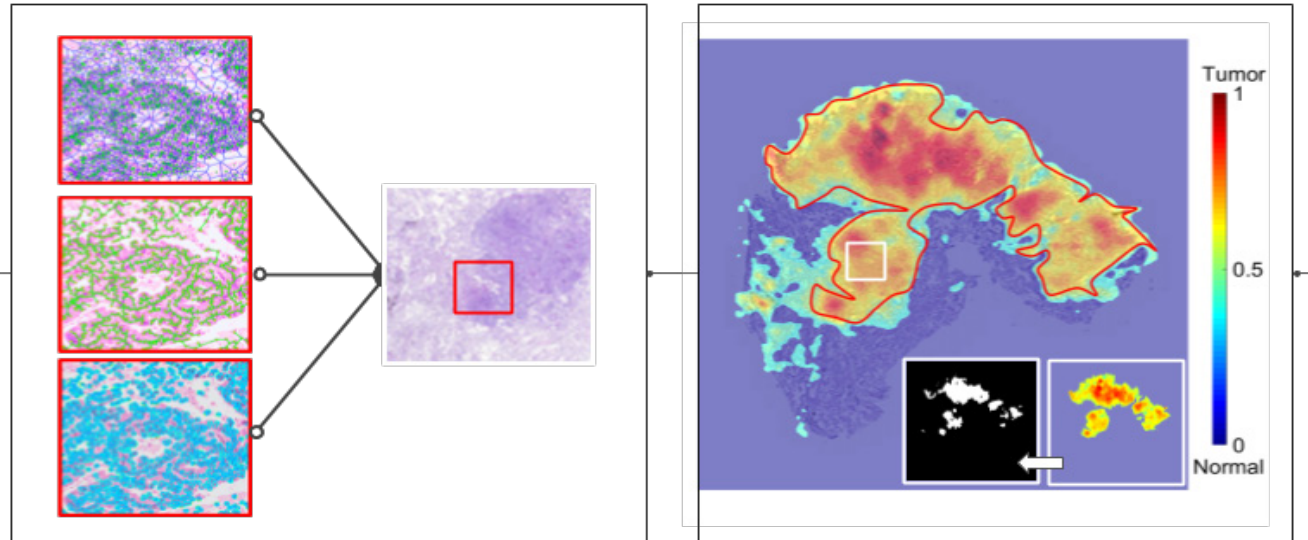
	73	46	14	3	0
High-Risk	73	46	14	3	0
Low-Risk	151	96	31	6	0



	76	39	9	2	0
High-Risk	76	39	9	2	0
Low-Risk	85	53	21	7	0



(a) automated tumor region prediction



IbRiS is prognostic and predictive for added benefit for adjuvant chemotherapy in early stage non-small cell lung cancer

Spatial arrangement of clusters of tumor infiltrating lymphocytes and cancer nuclei is predictive of recurrence in early stage non-small cell lung caner

Non-Recurrence

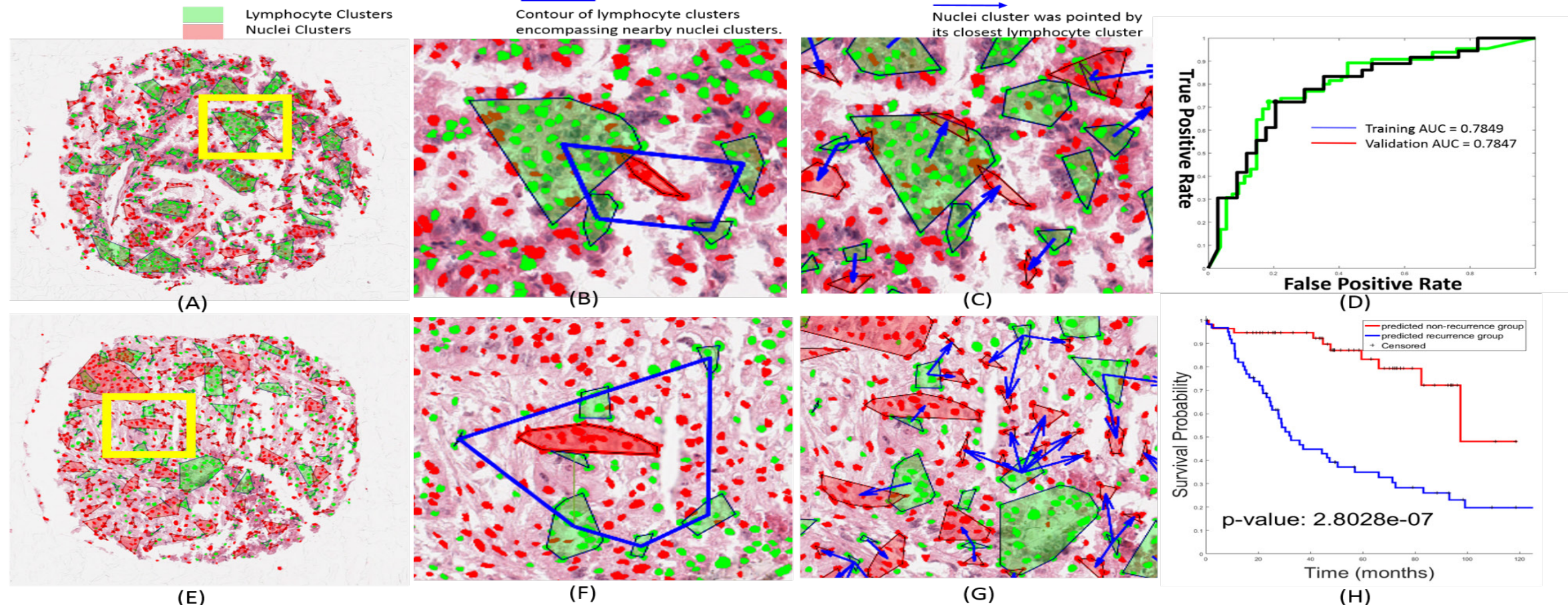
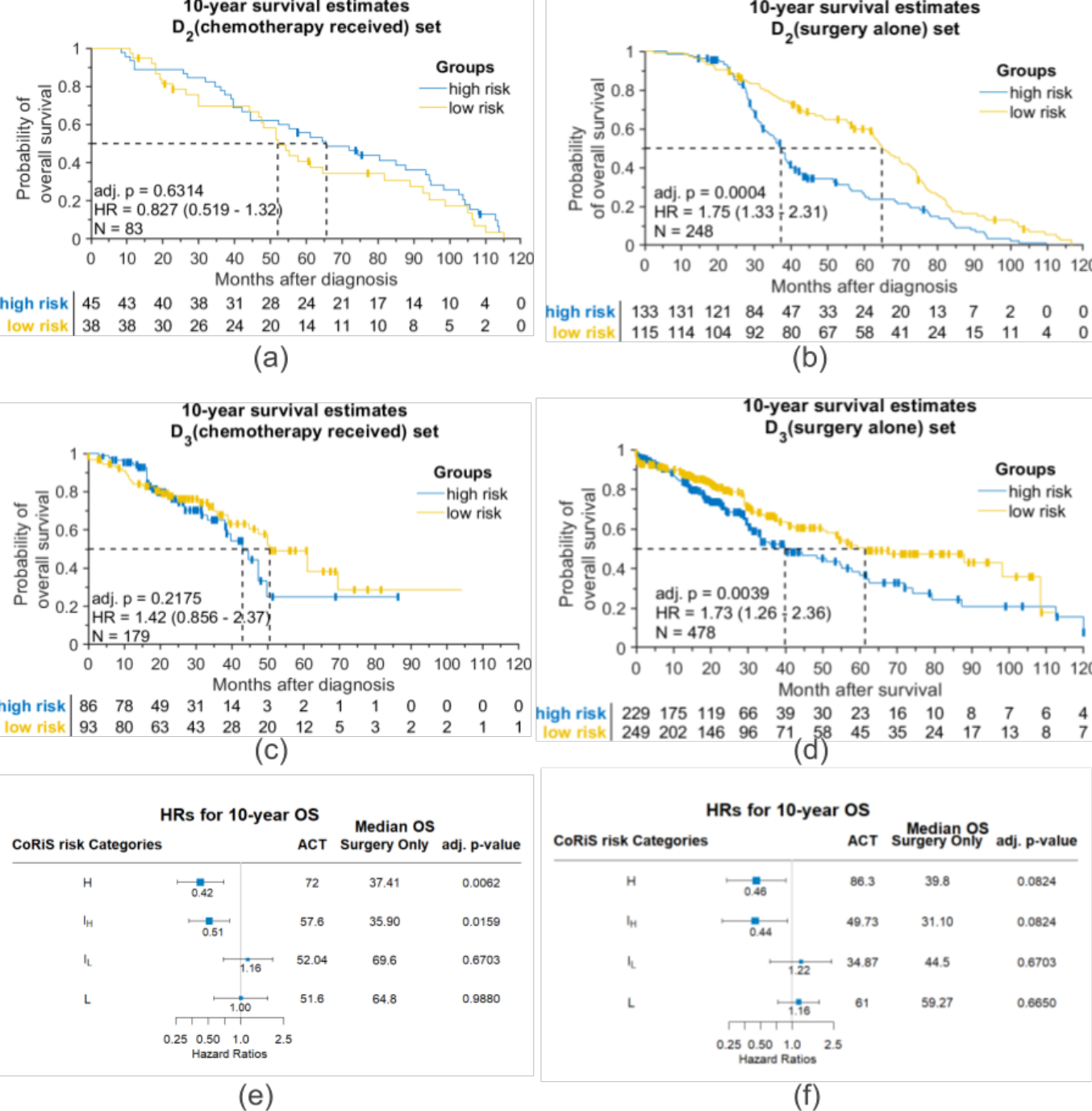


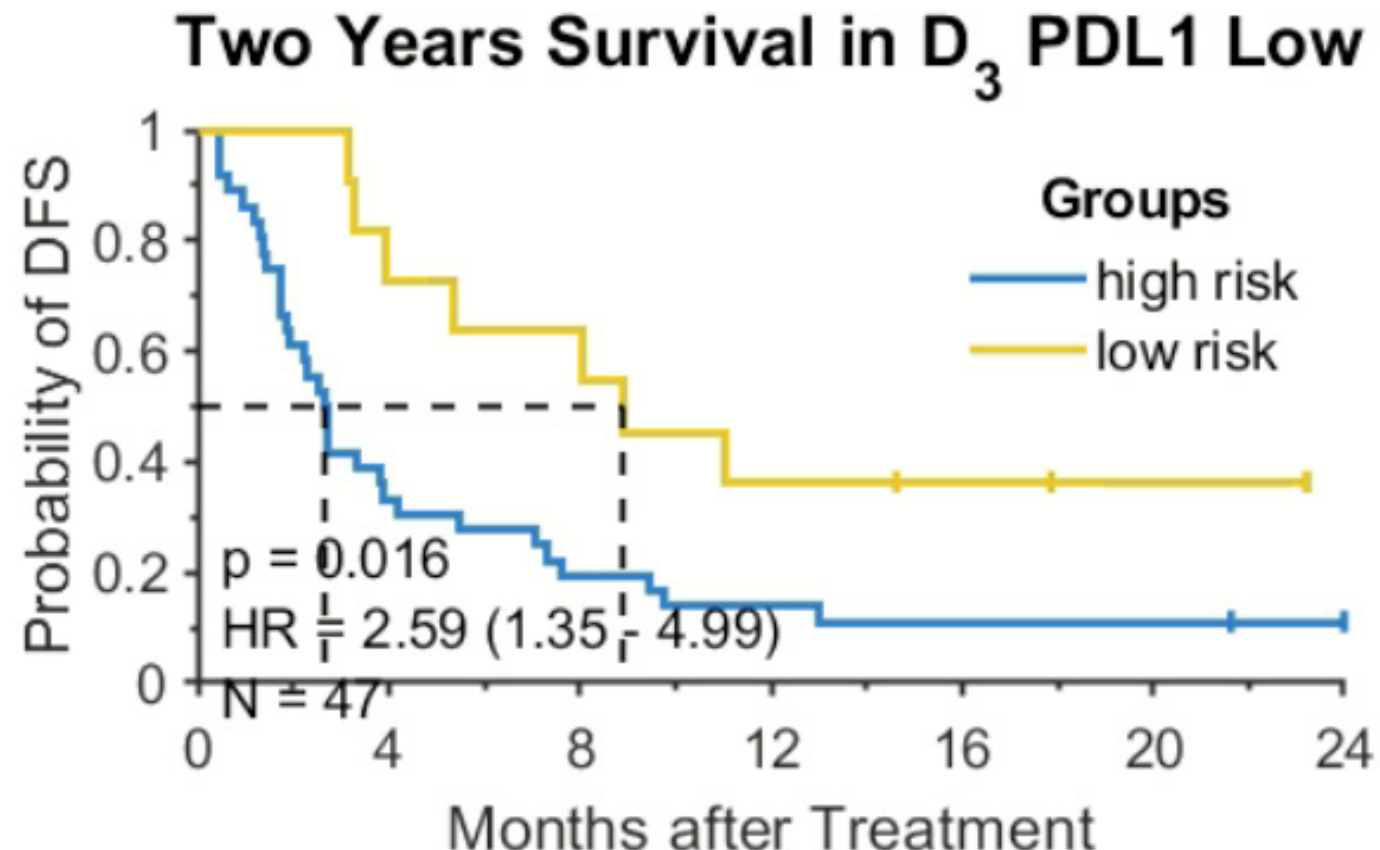
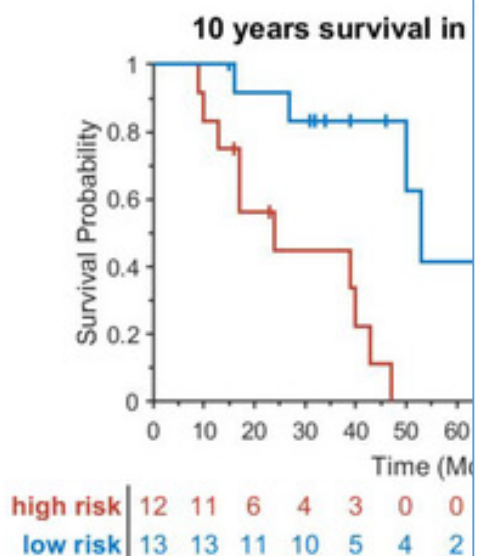
Figure 1. (A) Non-recurrent and (E) Recurrent NSCLC patient images. (A, E) TIL (green) and cancer nuclei cluster (red) construction, (B, F) number of proximal TIL clusters circumscribing each nuclear cluster, (C, G) Arrows show location of closest TIL cluster with respect to each cancer nuclei cluster, (D) receiver operating curve for both training and validation sets (AUC=0.78 for both sets) for the quadratic discriminant analysis in conjunction with the 12 most predictive features. (H) Kaplan-Meier curves showing separation between the recurrent and non-recurrent cases on the test set via the quadratic discriminant analysis in conjunction with the 12 most predictive features ($p < 10^{-7}$). Note: nuclei cluster are closely encompassed by proximal lymphocyte clusters for patients with better outcome (see area and vertex of blue contour in B and F); nuclei cluster are guarded tightly by surrounding lymphocyte cluster (see the arrow source point in C and G).

IbRiS is predictive of added benefit of adjuvant chemotherapy in early stage lung cancer

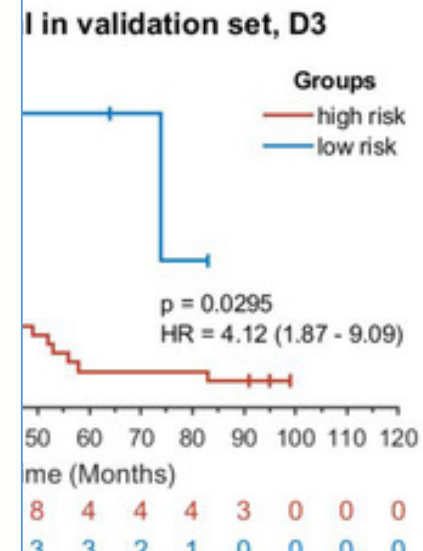


Kaplan-Meier plots showing predictive effect in CoRiS defined different risk of overall survival groups: (a) patients received adjuvant chemotherapy in D2; (b) patients only received surgery in D2; (c) patients received adjuvant chemotherapy in D3; (d) patients only received surgery in D3. Forest plots of different CoRiS defined risk of overall survival groups in (e) D2 and (f) D3.

Architecture of Tumor-Infiltrating Lymphocyte on H&E Slides Associated with Response and Outcome in IO Treated Lung Cancer

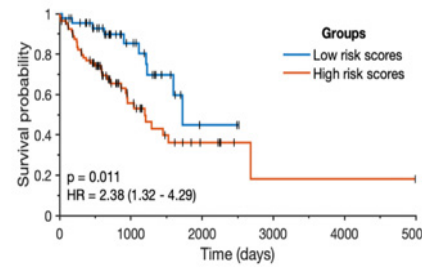
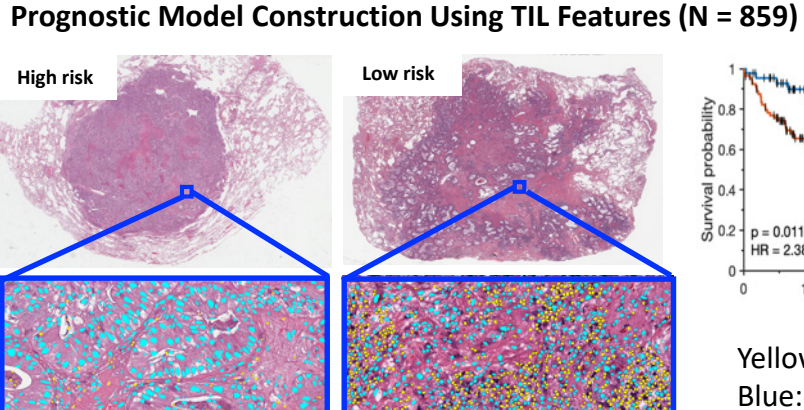


high risk	36	12	7	5	4	4	3
low risk	11	8	7	4	3	2	0

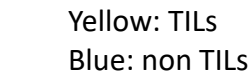
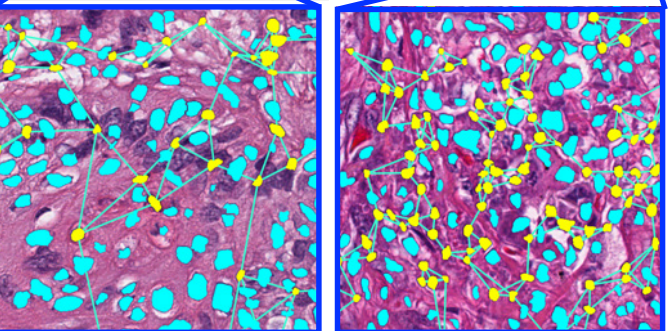
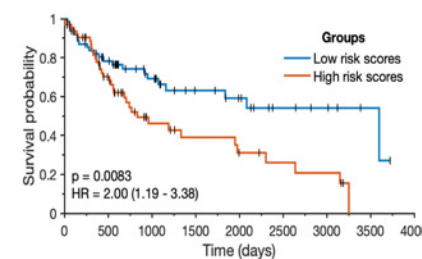
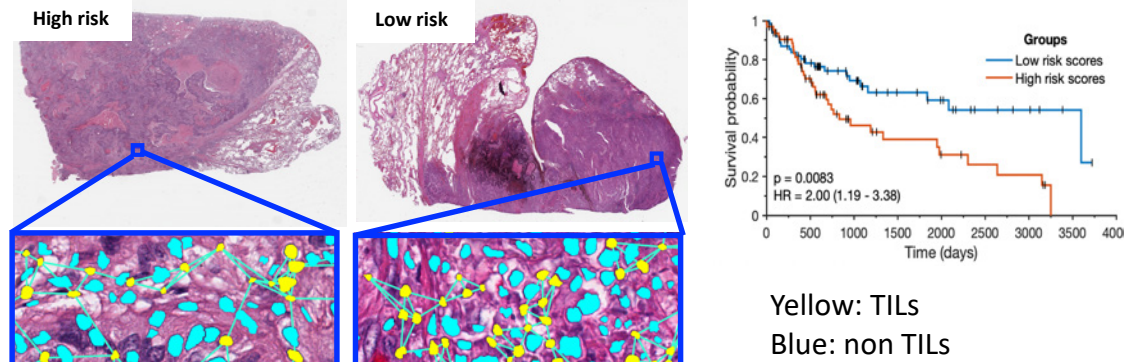


Computational Image Analysis of H&E and QIF Tissue Slides Reveals Morphologically and Molecularly Distinct Prognostic Patterns of Tumor Infiltrating Lymphocytes between Adenocarcinoma and Squamous Cell Carcinomas in Non-Small Cell Lung Cancer

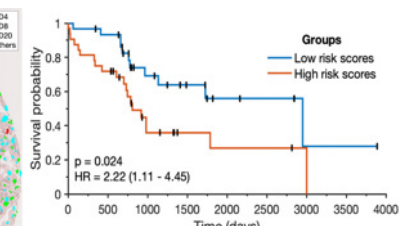
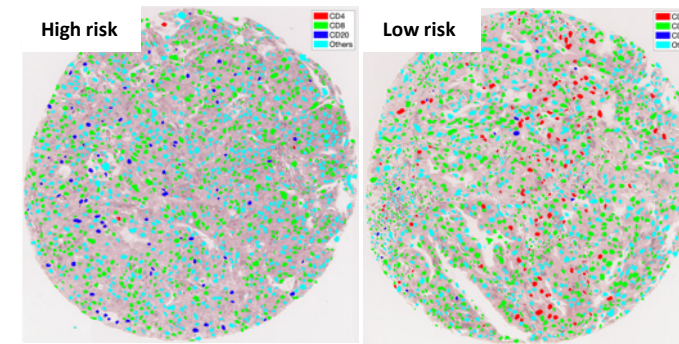
TIL density measures on LUAD



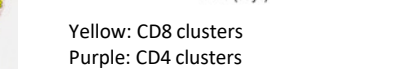
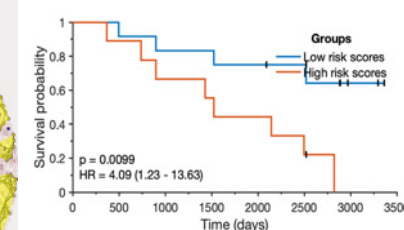
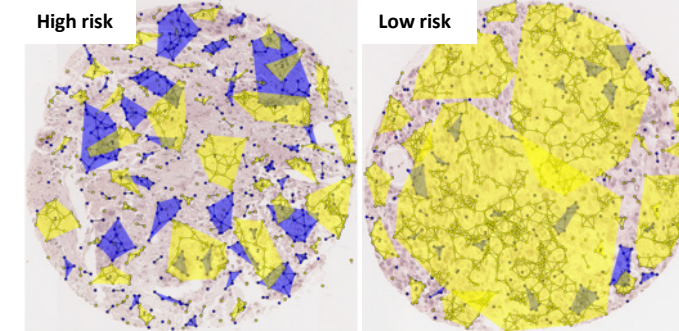
TIL spatial distribution on LUSC



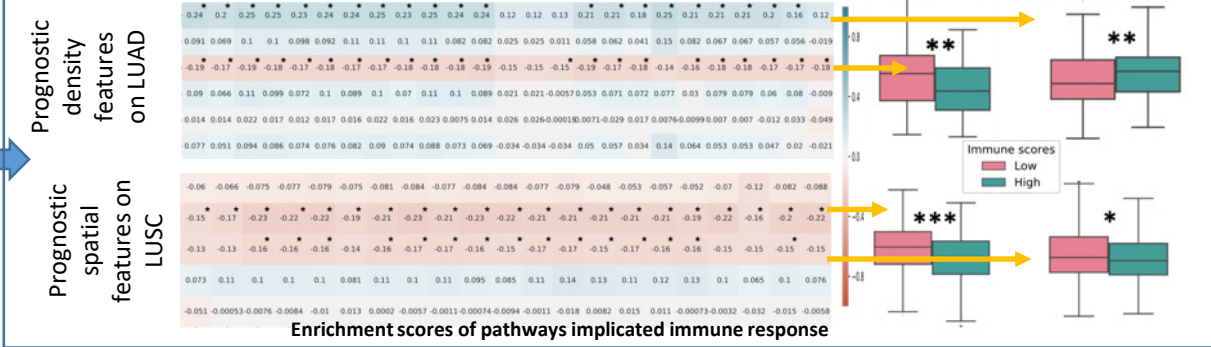
CD4+ density on LUAD



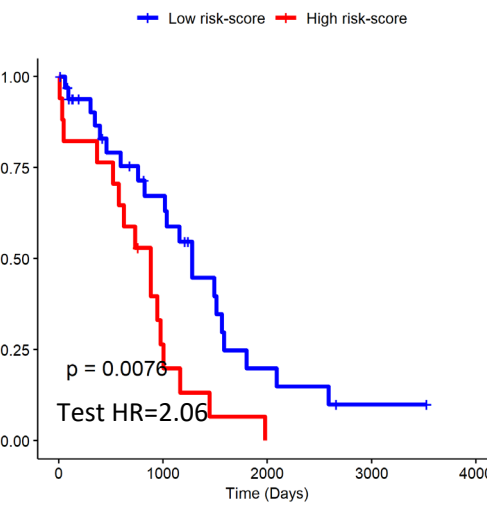
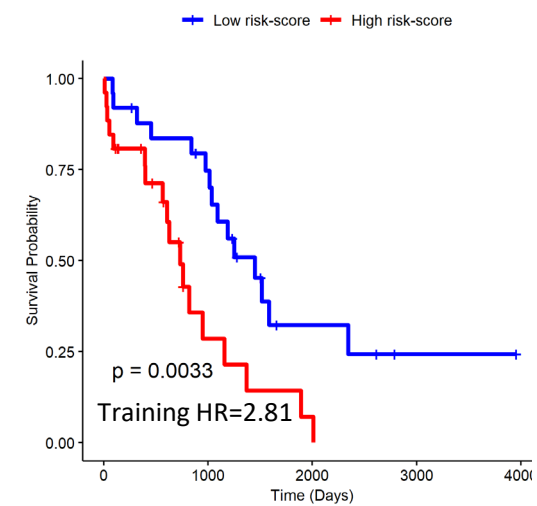
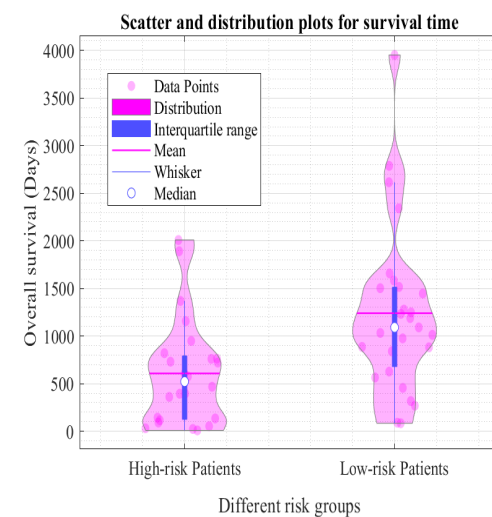
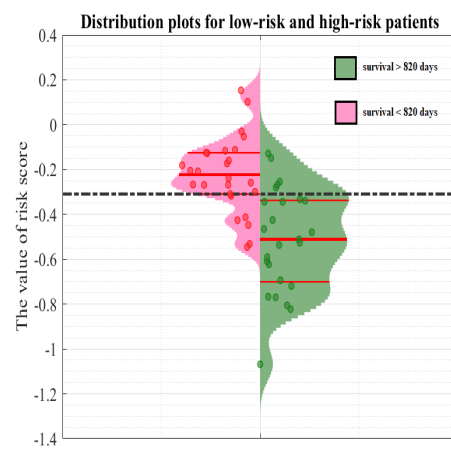
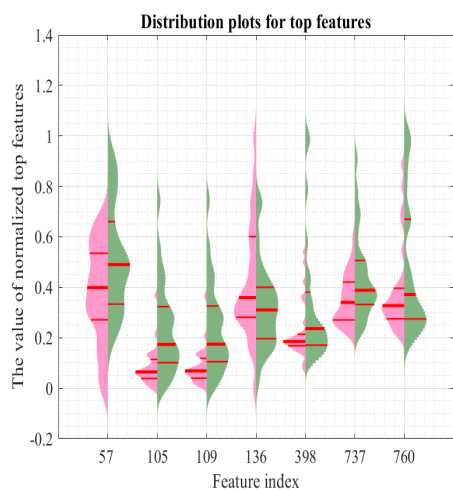
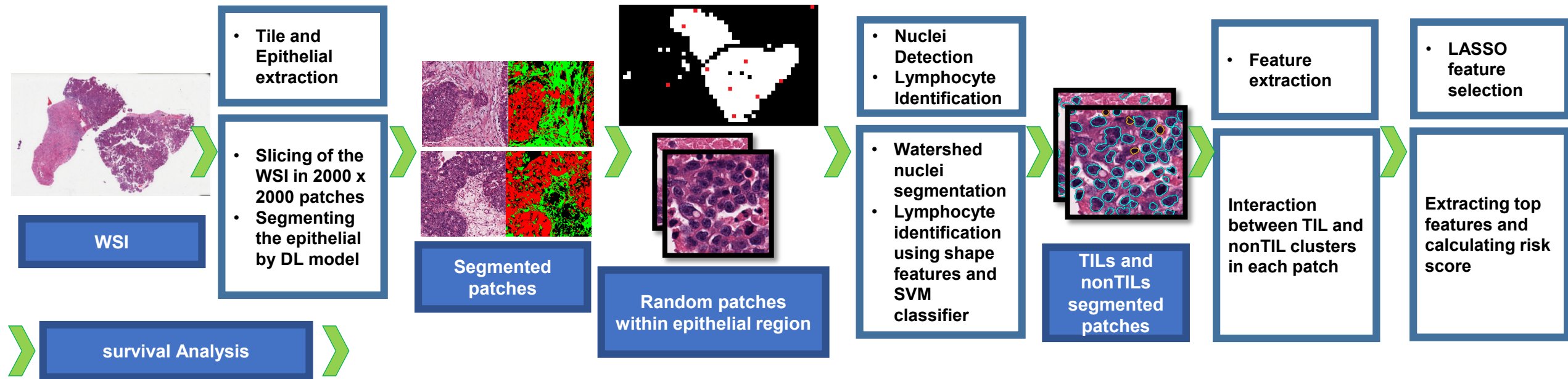
CD4+ vs CD8+ spatial interaction on LUSC



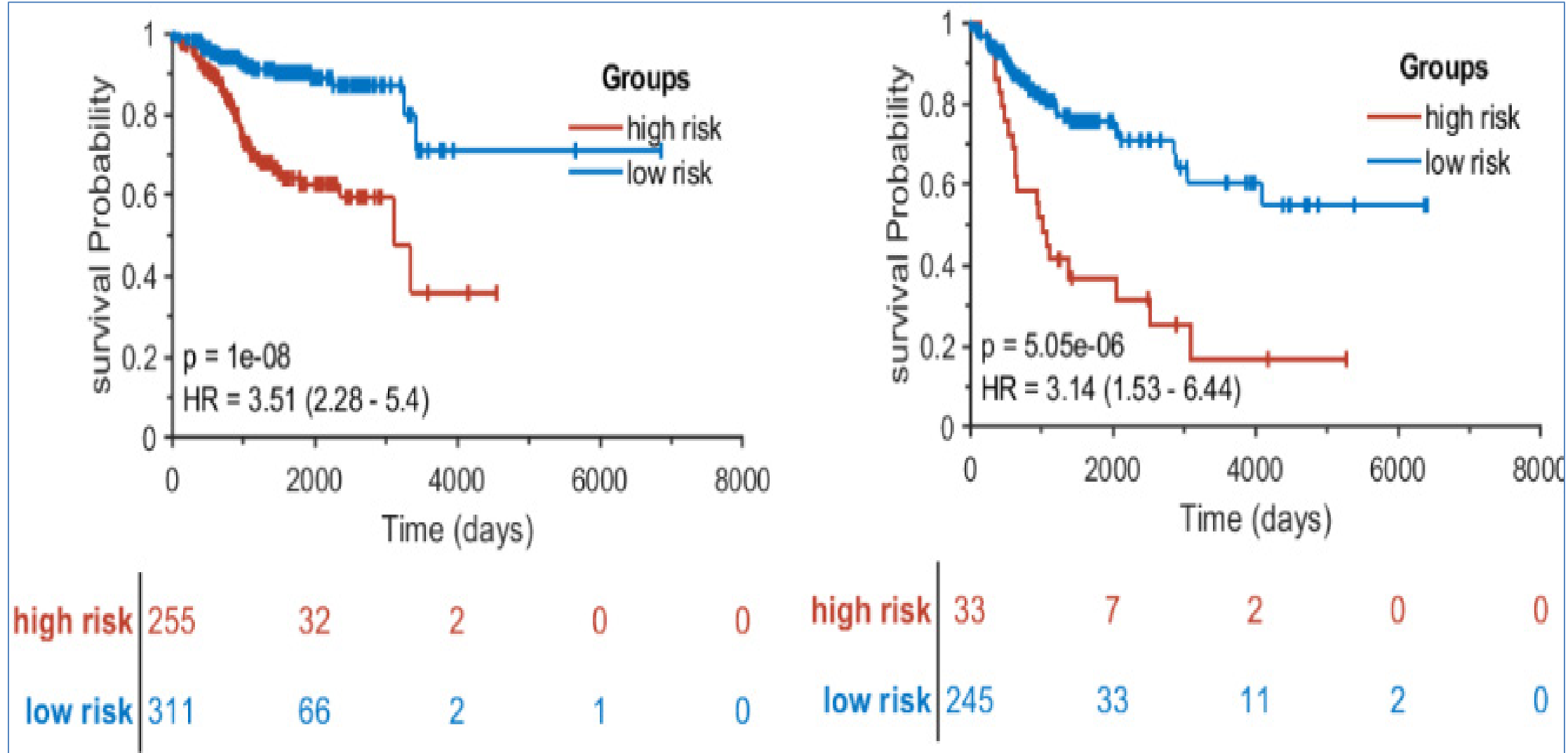
(N = 859) Association between Prognostic Signatures and 1) Biological Pathways 2) Immune Scores



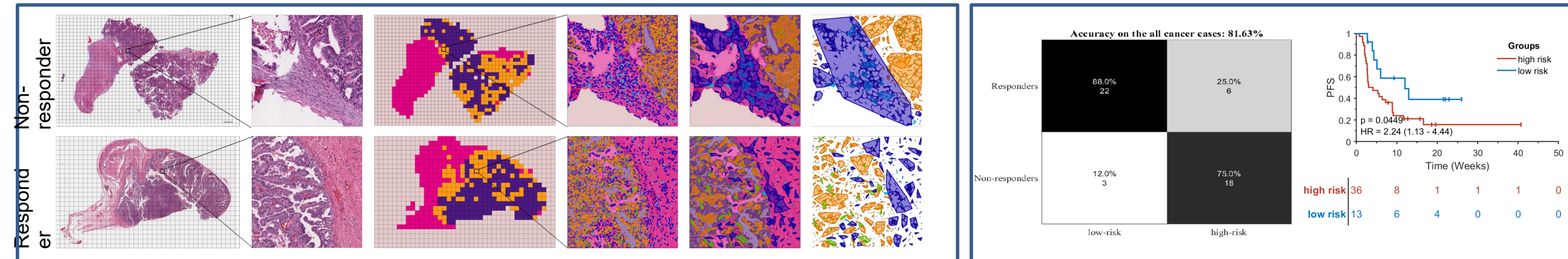
Predicting overall survival in Ovarian Cancer using SpaTIL



Predicting overall survival in Endometrial and Cervical Cancers using SpaTIL



Spatial arrangement of TILs for predicting response to IO in gynecological cancers



A. Representative patch of short- (top) and long-term survivor (bottom). (cyan: stromal TILs, blue: stromal non-lymphocyte cells, green: epithelial TILs, orange: cancer-cells)

In non-responders, the epithelial TILs are scarce, but the stromal compartment contains groups of stromal TILs (cyan), resulting in larger areas of cell cluster graphs. However, in responders, the presence of epithelial TILs dispersed among cancer cells caused highly fragmented cluster graphs.

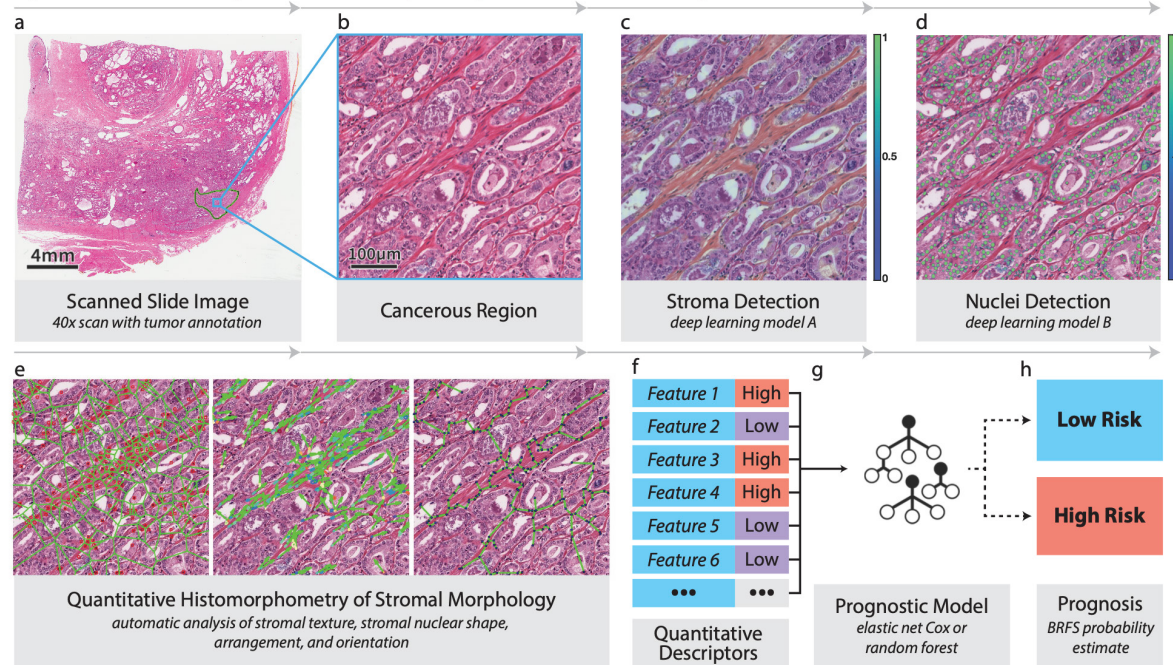
Takeaways

- Arrangement of cell families appeared significantly different between responders and non-responders. There are generally more evenly-distributed and smaller clusters in responders.
- Sub-visual cell arrangement could potentially be used to identify early clinical response before administrating therapy
- Imaging features could potentially identify patients who are likely to derive clinical benefit from immunotherapy beyond clinical data.

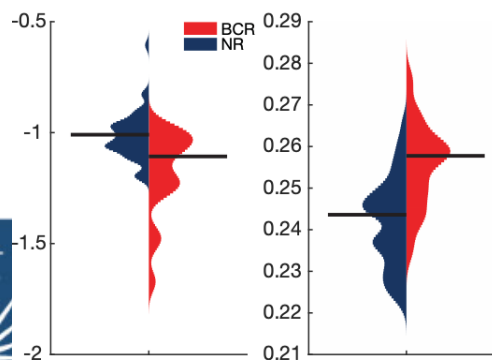
Confusion matrix and KM curves of high- (red) and low-risk groups (blue) in PFS of GC ICI-treated cohort ($N=49$, $HR=2.24$, $CI=[1.13-4.44]$, $p=0.045$). (epithelial ovarian cancer: 14, endometrial: 28, cervical cancer: 7)

Prediction of Prostate Cancer Recurrence across Racial Groups using Computer-Extracted Features from Stromal Regions of Radical Prostatectomy H&E Slides

Figure 1. Method: Stromal quantitative histomorphometry for cancer recurrence risk prediction.



d Shape Descriptors ($V_{T,AA}$)



e Texture Descriptors ($V_{T,AA}$)

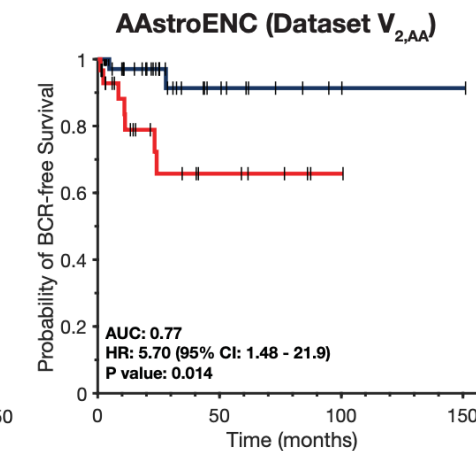
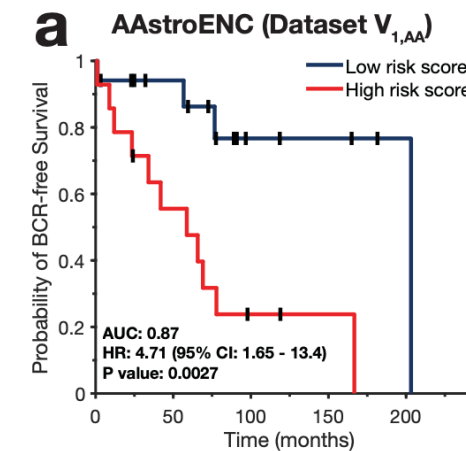
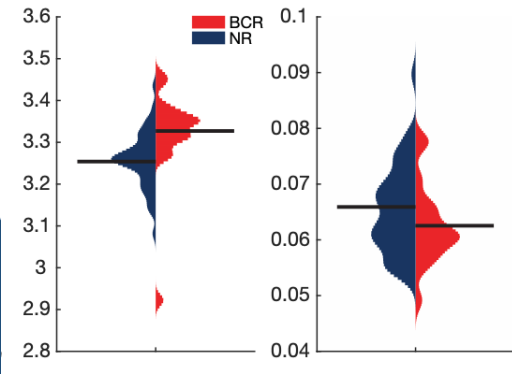


Figure 3. Association of stromal image features with IHC-derived tumor biomarker expression levels.

a

Marker Expression
immunohistochemistry

PTEN	TMPPSS2-ERG
PSMA	P-53
Racemase	C-MYC
Androgen Rec.	Ki-67
EZH2	Retinoblastoma

Stromal Features
quant. histomorphometry

Texture
Shape
Orientation
Arrangement

b

Biomarker-Correlated Stromal Descriptors

Biomarker	Stromal Feature	Corr.	P value	Prognostic?
Retinoblastoma	Shape: Mean Fract. Dimension	0.606	4.97E-04	Yes
TMPPSS2-ERG	Texture: Mean Info. Measure 1	-0.447	3.26E-02	Yes
Androgen Rec.	Shape: Mean Fract. Dimension	0.414	4.12E-04	Yes
Retinoblastoma	Shape: Mean Invar. Moment 2	-0.601	5.59E-04	No
PTEN	Shape: Fourier Descriptor 4	-0.623	7.56E-03	No
PTEN	Shape: Fourier Descriptor 3	-0.605	1.01E-02	No
ERG	Arrang: Triangle Area Disorder	-0.557	5.72E-03	No
C-Myc	Arrang: STDEV Edge Length	0.446	2.38E-03	No
	...			

Conclusion: A model trained on AA patients to distinguish BCR+/- performs better on the AA validation set than one trained on a mixture of AA+CA patients.

Computerized image analysis reveals differences in early stage ER+ breast cancer phenotype of South Asian and North American women

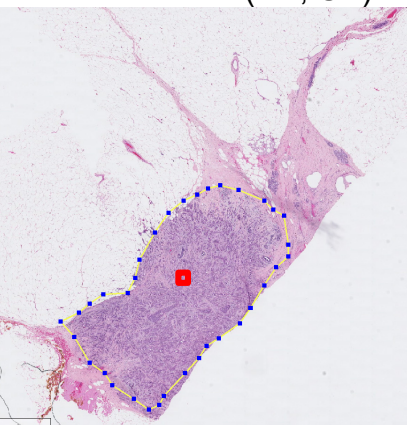
Unmet Clinical Need

- Racial/ethnic disparity in incidence and mortality in breast cancers.
- Indian women more likely to be diagnosed with advanced breast cancer despite lower incidence than American women.
- The studies of digital pathology in breast cancer prognosis were mostly focused on American women.

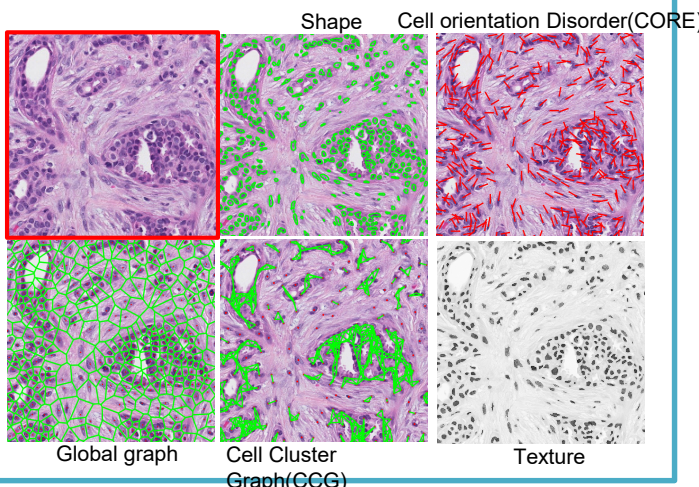
Methods and Results

Data Description

South Asian (SA, Indian): N=69
North American (NA, US): N=121



Extraction of nuclear morphological features



Model construction on training set

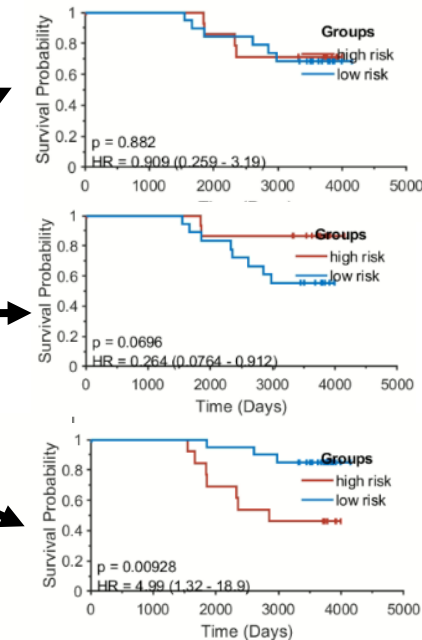
Validation on SA in testing set

Model trained with North American (MNA)

Model trained with North American + South Asian (MNA+SA)

Model trained with South Asian(Msa)

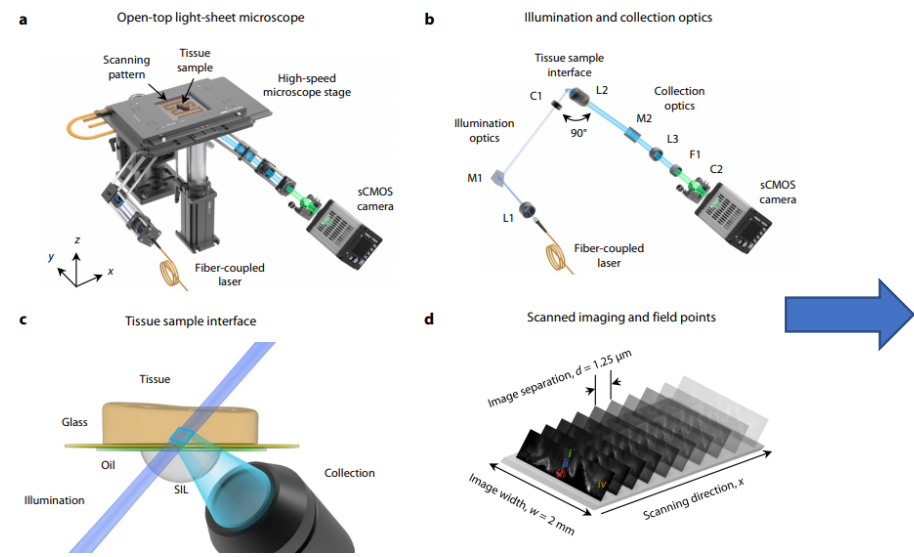
Model validation on South Asian



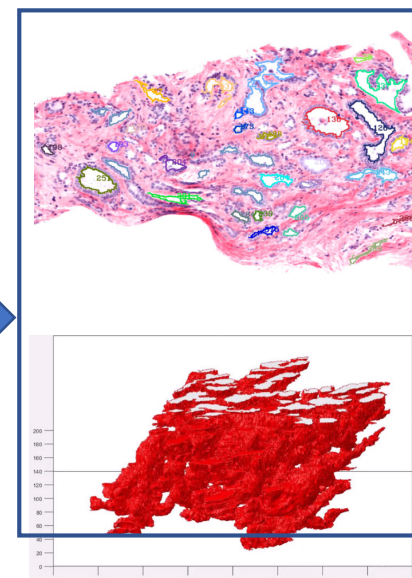
Take away:

Prognostic ability of the computational pathology based models for South Asian women with breast cancer could be significantly improved by taking into account of population-specific information.

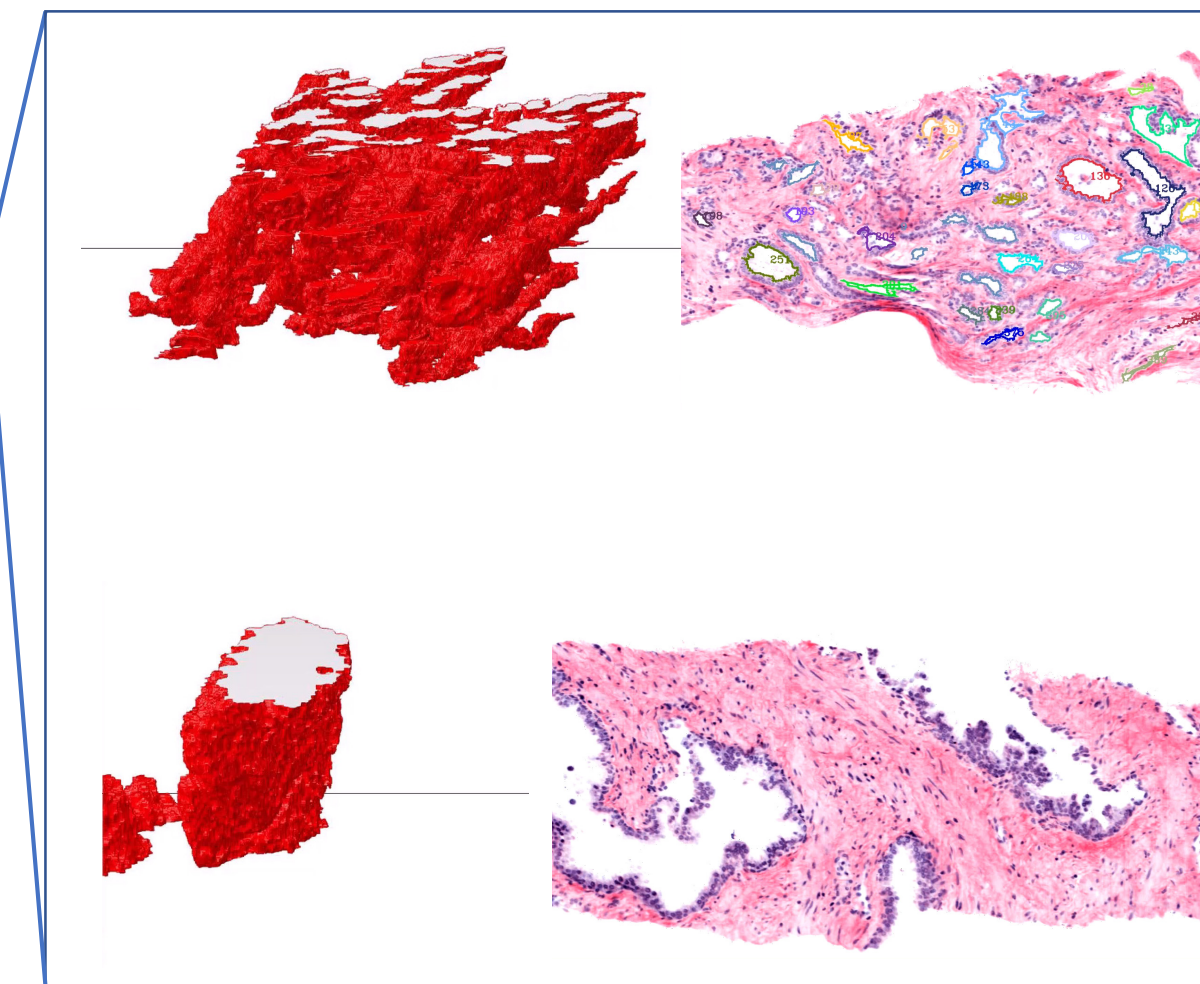
3D lumen-feature extraction from prostate pathology images of light-sheet microscopy for better Gleason score definition



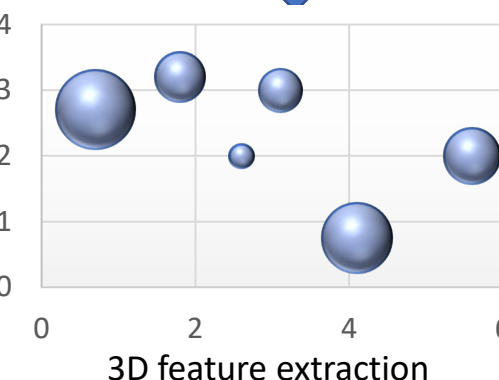
3D image acquisition from light-sheet microscopy [1]



3D lumen segmentation



Better Gleason score definition in 3D space [2]



[1] Glaser A. K., et al., Light-sheet microscopy for slide-free non-destructive pathology of large clinical specimens, Nat. Biomed. Eng. 2017, 1, 0084.

[2] Image is obtained from the link: <https://www.prostateconditions.org/about-prostate-conditions/prostate-cancer/newly-diagnosed/gleason-score>

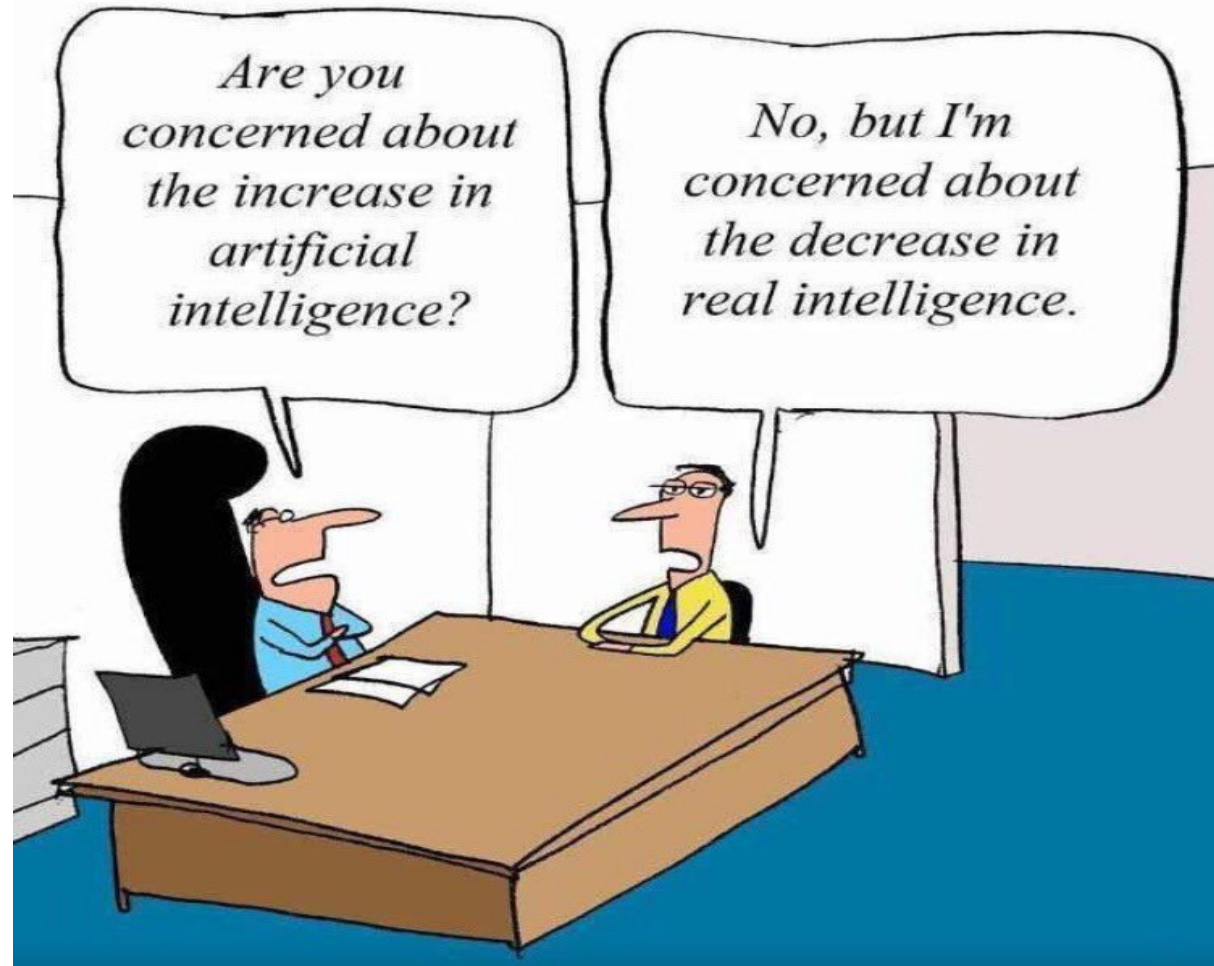
Take Away

- **Computational Analytics with routine imaging** could help address questions in precision medicine, specifically prognosis and predicting response to therapy
- **Low cost computational diagnostics**
- **Global impact**, especially **low and middle income** countries.
- Multi-scale disease associations, looking to establish the morphologic and molecular basis of the imaging features. Need an intuitive basis to drive clinical adoption

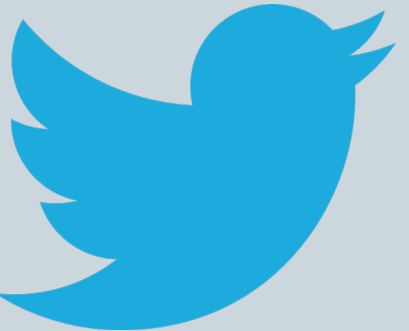
- National Cancer Institute:
U24CA199374-01,
R01CA202752-01A1,
R01CA208236-01A1, R01
CA216579-01A1, R01
CA220581-01A1
- National Center for Research Resources under award number:
1 C06 RR12463-01
- the DOD Prostate Cancer Synergistic Idea Development Award (PC120857); the DOD Lung Cancer Idea Development New Investigator Award (LC130463), the DOD Prostate Cancer Idea Development Award; the DOD Peer Reviewed Cancer Research Program W81XWH-16-1-0329
- the Ohio Third Frontier Technology Validation Fund
- the Wallace H. Coulter Foundation Program and the Clinical and Translational Science Award Program (CTSA) at Case Western Reserve University.

Acknowledgements





← **Anant Madabhushi**
2,015 Tweets



Anant Madabhushi
@anantm
Artificial Intelligence, Cancer imaging, Digital pathology, radiomics, pathomics, precision medicine

Edit profile

@anantm